Science and Applied Sciences Faculty

Department of Mechanical Engineering

END OF STUDY PROJECT

Presented for the award of the Master's Degree
Specialty: Mechanical Engineering
Option: Energy

THEME

Thermal Analysis of a Firefighter Protective Body-Clothing assembly

Realized by:

Imad Eddine Doukari

Nasr Eddine Siar

Supported on 28/06 /2025 before the jury composed of

Dr. Sofiane Aberkane	University of Bouira - President
Dr. Chafik Bensalem	University of Bouira -Supervisor
Dr. Anis Aghbari	University of Bouira -Examiner

Academic year : 2024/2025

Dedication

This final project is dedicated with deepest gratitude and heartfelt appreciation to those who have stood beside me throughout this academic journey.

To my beloved parents, whose love, prayers, and unwavering belief in my potential have been my greatest source of strength—thank you for every sacrifice you made to provide me with the opportunity to pursue my education. Your words of encouragement and constant support have shaped my character and fueled my determination during the most challenging moments.

To my family, who have been a continuous pillar of strength, thank you for your patience, understanding, and faith in me, even during the times when I doubted myself. Your emotional and moral support carried me through long nights and difficult decisions.

To my professors and academic advisors, thank you for your valuable guidance, mentorship, and for sharing your knowledge with passion and dedication. Your constructive feedback and continuous encouragement have greatly contributed to the development and completion of this project.

To my dear friends and colleagues, who have been companions through every step of this academic path—thank you for the camaraderie, laughter, and the many moments of mutual support. Our shared experiences enriched my journey in ways that go far beyond academics.

Finally, I dedicate this work to all the dreamers and learners who believe in the power of persistence and education. May this project serve as a humble contribution to the field and as a reminder that with dedication, patience, and support, even the most ambitious goals are achievable.

Imadeddine.

Dedication

With deepest gratitude and heartfelt appreciation, I dedicate this work to those who have been my unwavering support throughout this journey.

To my beloved parents—your unconditional love, prayers, and belief in me have been the foundation of my strength. Your sacrifices and constant encouragement have shaped not only this academic achievement but the person I have become. For everything you have done, I am eternally grateful.

To my family, thank you for being my source of resilience. Your understanding, patience, and faith in me—even when I doubted myself—carried me through the most difficult times.

To my professors and academic mentors, your wisdom, guidance, and dedication have left an indelible mark on my learning journey. Your support has inspired me to push boundaries and pursue excellence.

To my friends and colleagues, thank you for walking beside me through every challenge and every victory. The shared experiences, laughter, and solidarity made this path more meaningful.

Lastly, this work is dedicated to all the dreamers, learners, and believers in the power of persistence. May it serve as a humble reminder that with commitment, support, and faith, no goal is beyond reach.

Nasereddine.

Acknowledgment

First and foremost, we express our deepest gratitude to Almighty Allah for granting us the strength, determination, and guidance to successfully carry out this academic endeavor.

We are profoundly thankful to our supervisor, **Dr. Bensalem chafik**, for his exceptional patience, insightful guidance, and continuous support throughout the course of this research. His encouragement and expertise have been instrumental in the completion of this project.

We also extend our sincere thanks to **Dr. messai**, , for his valuable advice, thoughtful suggestions, and generous guidance, all of which greatly enriched the quality of our work.

Our heartfelt appreciation goes to the distinguished members of the jury for kindly accepting to evaluate our work and for their constructive feedback. We are equally grateful to all the professors who have contributed to our academic and personal growth throughout our years of study.

Finally, we would like to express our deepest appreciation to our families, whose constant support, encouragement, and unwavering belief in us provided the emotional foundation that helped us persevere through every challenge faced during this journey.

Abstract

Fires are among the major causes of fatalities and injuries. As statistical survey conducted by the international association of fire and rescue services (CTIF) revealed several injuries and deaths between the firefighters, over 56 countries. During rescue actions, firefighters can be exposed to multiple fire conditions including flashovers and backdrafts. Accordingly, the performances of the protective clothing are the key demands for any fire safety strategy or fabrics manufacturing. In this context, several unexpected burn injuries were noted on firefighters bodies, despite the consistency of the protective clothings. Developing thermophysical models for the clothing-skin interaction seem as a challenging task and a promising way for the firefighting community. The present work is an attempt to predict the spatial and temporal evolution of the temperature in the body-clothing assembly. The algebraic 1D model is based a heat transfer balance accounting for radiation-convection-conduction on each fabrics and skin layer.

Keywords: Firefighter clothing, Thermal characterization, Biothermics, Burn injuries.

Résumé

Les incendies sont l'une des principales causes de décès et de blessures. Une enquête statistique menée par l'Association internationale des services d'incendie et de secours (CTIF) a révélé plusieurs blessures et décès parmi les pompiers dans plus de 56 pays. Lors des interventions de secours, les pompiers peuvent être exposés à de multiples conditions d'incendie, notamment des embrasements fulgurants et des refoulements d'air. Par conséquent, la performance des vêtements de protection est une exigence clé de toute stratégie de sécurité incendie ou de fabrication de tissus. Dans ce contexte, plusieurs brûlures inattendues ont été constatées sur le corps des pompiers, malgré la cohérence des vêtements de protection. Le développement de modèles thermophysiques pour l'interaction vêtements-peau semble être une tâche difficile et une voie prometteuse pour la communauté des pompiers. Ce travail vise à prédire l'évolution spatiale et temporelle de la température dans l'ensemble corps-vêtements. Le modèle algébrique 1D repose sur un bilan de transfert thermique prenant en compte le rayonnement, la convection et la conduction sur chaque tissu et chaque couche de peau.

Mots-clés : Vêtements de pompier, Caractérisation thermique, Biothermie, Brûlures.

ملخص

تُعدّ الحرائق من الأسباب الرئيسية للوفيات والإصابات. وقد كشف مسح إحصائي أجرته الرابطة الدولية لخدمات الإطفاء عن العديد من الإصابات والوفيات بين رجال الإطفاء في أكثر من 56 دولة. وخلال عمليات الإنقاذ، قد يتعرض رجال والإنقاذ الإطفاء لظروف حريق متعددة، بما في ذلك الوميض الحراري والتيارات الهوائية العكسية. وبناءً على ذلك، يُعدّ أداء الملابس الواقية من المتطلبات الأساسية لأي استراتيجية للسلامة من الحرائق أو تصنيع الأقمشة. وفي هذا السياق، لوحظت العديد من إصابات الحروق غير المتوقعة على أجساد رجال الإطفاء، على الرغم من تناسق الملابس الواقية. ويبدو تطوير نماذج حرارية فيزيائية للتفاعل بين الملابس والجلد مهمةً صعبةً ووسيلةً واعدةً لمجتمع مكافحة الحرائق. ويهدف هذا العمل إلى التنبؤ بالتطور المكاني والزماني لدرجة الحرارة في تركيبة الملابس والجسم. ويستند النموذج الجبري أحادي الأبعاد إلى ميزان انتقال الحرارة الذي يأخذ في الاعتبار الإشعاع والحمل الحراري والتوصيل على كل قماش وطبقة من الجلد.

الكلمات المفتاحية: ملابس رجال الإطفاء، التوصيف الحراري، المعالجة الحرارية الحيوية، إصابات الحروق.

Table of Contents

List of figures

List of figures

List of Tables

Nomenclature

T	Temperature	K or °C
Tamb	Ambient temperature	K
Tm	Metabolic reference temperature	K
δ	Layer thickness	mm
λ	Thermal conductivity	W/m·°C
ρ	Density	kg/m³
Cp	Specific heat capacity	J/kg·K
α	Absorptivity	
ε	Emissivity	
h	Convective heat transfer coefficient	W/m²·K
Gf	Radiative heat flux	W/m²
Gm	Metabolic heat generation	W/m²
Gevap	Heat flux due to evaporation	W/m²
q	Heat flux	W/m²
k	Thermal conductivity (alternative symbol for λ)	W/m·K
t	Time	s
$\dot{Q}$	Heat transfer rate	W
A	Surface area	m²
Ep	Air gap thickness between layers	m
ωb	Blood perfusion rate	1/s
Qm	Metabolic heat generation rate	W/m³
Cb	Blood specific heat capacity	J/kg·K
Tb	Blood temperature	K or °C
Tvenous	Venous blood temperature	K or °C
Tarterial	Arterial blood temperature	K or °C
Δt	Time step used in numerical integration	s
k1,k2,k3,k4	Runge-Kutta intermediate coefficients	
Frad	Radiative heat flux component	W/m²
Fconv	Convective heat flux component	W/m²
Fcond	Conductive heat flux component	W/m²

Nomenclature

σ	Stefan-Boltzmann constant	$W/m^2 \cdot K^4$
Tskin	Skin temperature (surface or internal)	K or °C
ISO 15025	International test standard for limited flame spread of protective clothing	Test Standard
CNTC	Centre National du Textile et du Cuir (Boumerdes, Algeria) where experimental tests were done	Institution
COMSOL	Commercial multiphysics simulation software used for some comparative numerical studies	Software
MATLAB	Computational software used for simulating heat transfer and protective clothing performance	Software
RK4	Runge-Kutta 4th order numerical method	Numerical method

General Introduction

General Introduction

Firefighters are usually the first-line responders in emergency situations of fire, explosion, chemical spillage, and other hazardous situations. Of these, fire situations pose some of the most dangerous occupational hazards due to the very intense thermal conditions to which firefighters are exposed. In such operations, firefighters are subjected to high intensities of radiant, convective, and conductive heat, which can easily cause grave injury or fatality if not properly shielded. Consequently, firefighters' own life and health largely depend on the performance of his/her personal protective equipment (PPE), especially thermal protective clothing, which is the main barrier against exterior sources of heat.

The importance of high-performance thermal protective apparel cannot be emphasized enough. Not only does it serve as the outer shield from the elements of fire and heat, it also protects against burns, heat sickness, and other thermal-induced harm. But if the protective apparel does fail—because it was poorly designed, made of unsuitable materials, or weakened from extended use—the outcome can be of dire consequences. Injuries from such incidents tend to be life-threatening in nature and can have long-term health consequences, disability, or be lethal. In addition, the lack of adequate protection for firefighters can also lead to more property loss and loss of operational efficiency in responding to emergency situations.

Every year, many firefighters worldwide get injured from fires in spite of wearing protective attire, testifying to an ongoing mismatch between existing PPE technology and the harsh fire conditions experienced in the line of duty. The occurrence of such accidents indicates the need for innovation in the engineering and designing of thermal protective apparel. New-generation fire brigades require more than just fire-resistance in protective clothing; it should be resistant against multiple modes of heat transfer at once—conduction from contact with hot surfaces, convection from hot gases or hot air, and radiation from hot objects or fire. Furthermore, environments for firefighting tend to be multifaceted and unpredictable. Beyond thermal hazards,

firefighters are subjected to a broad array of other hazards, including toxic gases, biological agents, structural collapse and its attendant physical trauma, and radiation. Not withstanding the complexity of the situation, thermal exposure is still the most common and direct hazard in wildland and structural fire situations. For example, structural fires can yield hot steam, volatile gases, charred materials, and molten material—all of which add to higher thermal loads. Even in cases where suppression with water is unavoidable, the water usually becomes superheated steam and enhances the risk of burn injury due to its higher thermal retention as opposed to dry air.

Considering the intricacy and severity of these issues, it is critical to evaluate and enhance the thermal protective performance of firefighter apparel in an organized way. Present-day PPE fails short of responding to actual fireground environments, specifically extended thermal exposure, steam burns, and sudden thermal flux. Although advances have been made in material science and garment technology, protection from present-day ensembles continues to be less than optimal in some respects.

The objective of the research is to critically analyze the thermal protective function of the present-day firefighter clothing systems. Through the execution of experimental testing and examination of state-of-the-art technology in textile technology, the research delves into what has been lacking in terms of protection and suggests possible solutions for enhanced thermal performance. The ultimate goal is to develop better design specifications and functionality requirements for protective firefighter clothing to promote improved survivability and performance in high-threat fire situations.

As part of this research effort, the research makes an overall contribution to occupational safety and health by providing useful insights into reducing injury frequency through the implementation of novel protective systems, enhancing emergency response performance, and ensuring firefighters' overall physical health across the world. [1]

This study has been organized into 5 major chapters:

●Chapter 01: Technological study.

●Chapter 02: State of the art.

●Chapter 03: Experimental tests.

●Chapter 04: Formulation and thermal balance equations.

●Chapter 05: Results and discussion / Parametric analysis and cases study.

Chapter I

Technological Study

I. Chapter 01 : Technological study

1. Introduction

Firefighting is a very risky profession, and the staff is subject to many hazards. Thermal hazards represent the most frequent among them, and they result from many sources, such as conduction, convection, hot fluids, steam, and contact with hot surfaces. Familiarization with the various categories and classes of fires, firefighting activity, and exposure hazards, as well as with the thermal balance of the body, is necessary in order to set up effective protection methods and habits. [2]

2. Fire Types and Classification

Fires can be categorized by the nature of the material that is being burned. The primary classifications are:

• Class A: Class A fire is made up of regular combustibles, such as fabric, paper, and wood. [3]

• Class B: Fires involving flammable liquids such as gasoline, oil, and alcohol.

Class C: Fires that occur with electrical equipment that is energized. [4]

• Class D: Burning of flammable metals, e.g., magnesium, titanium.

• Class K: Fires caused by cooking oils and fats. [5]

Each class has a range of challenges and necessitates a range of extinguishing techniques. A water application in Class B fire, for example, accomplishes nothing but propagates the flammable liquid, making the fire worse. Class C fire necessitates the use of non-conducting fire-extinguishing media so that electrical shock is not initiated.

CLASSES OF FIRES	TYPES OF FIRES	PICTURE SYMBOL
A	Wood, paper, cloth, trash & other ordinary materials.	
B	Gasoline, oil, paint and other flammable liquids.	
C	May be used on fires involving live electrical equipment without danger to the operator.	
D	Combustible metals and combustible metal alloys.	
K	Cooking media (Vegetable or Animal Oils and Fats)	

Figure I-1 : Fire Types and Classification**.** [6]

3. Firefighter's Activities and Exposure Risks

Firefighters carry out a variety of functions that subject them to numerous hazards:

• Fire Suppression : Fire in the surrounding area exposes firefighters to heat, smoke, and deadly gases. Heat from the area may cause heat stress, burns, and respiratory problems. Structural collapse is a serious physical hazard. [6]

• Rescue Operations : Going into fire or structurally damaged buildings in an attempt to rescue people exposes them to hazardous situations, exposes them to more risk from falling debris, explosions, or fire changes. [7]

• Hazardous Materials Response : Firefighters typically respond to the scene in cases of chemical, biological, nuclear, and radiological material incidents. These substances expose individuals to health risks, both short-term and long-term, in the form of respiratory disease and cancer. [8]

• Wildland Firefighting : Woodland and grassland firefighting is also subject to certain special difficulties, such as rough terrain, uncontrollable fire behavior, and prolonged heat and smoke exposure. The physical and environmental conditions tend to cause excessive heat and smoke sickness. [9]

The cumulative effect of all the above-mentioned exposures may result in long-term health issues. Fire fighting activity also correlates to hyperthermia, dehydration, and breathing issues, and some cancer.

Figure I-2 :Firefighter Activities and Exposure Risks. [11]

4. Composition of the skin of the organism

The skin is the largest organ in the human body, and it is the body's first line of defense against external dangers like heat, fire, and chemicals. The skin consists of three primary layers, and all play important roles in the areas of protection, sensation, and regulation of temperature.

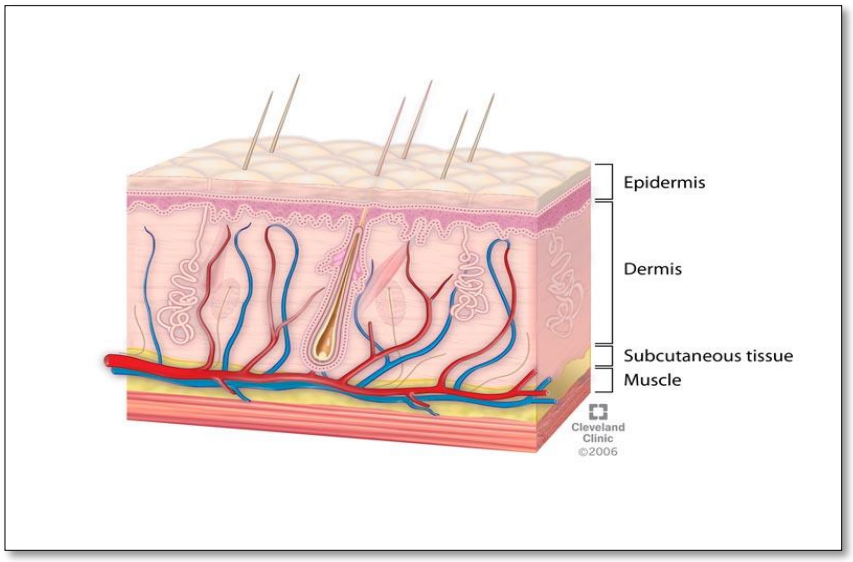

Figure I-3 : Composition of the skin of the organism. [12]

3.1. The Three Layers of Human Skin

3.1.1. Epidermis (Outer Layer):

The epidermis is the outermost, stratified, squamous epithelium that is composed mainly of keratinocytes and also dendritic cells (melanocytes, Merkel cells, and Langerhans cells). The epidermis is divided into four layers by the morphology of the type of keratinocyte and the degree of differentiation into cornified cells (the most superficial is the stratum corneum).

3.1.2. Dermis (Middle Layer):

The middle layer made up basically of collagen and amorphous connective tissue with nerve and vascular networks, epidermal appendages, fibroblasts, macrophages, and mast cells.

3.1.3. Hypodermis (Subcutaneous Tissue):

The hypodermis, which is also known as the subcutaneous tissue, is a real endocrine organ consisting of lobules of adipocytes separated by septa composed of collagen and blood vessels. [10]

5. Thermal Balance of the Human Body

Maintaining thermal equilibrium is crucial to the health and well-being of humans. The body preserves core temperature by sweating and the control of the flow of the blood. However, in warm climatic situations, the body's mechanisms are put under pressure, leading to heat illness

• Heat Cramps: Muscle cramps resulting from electrolyte imbalances through heavy sweating.

• Heat Exhaustion: A syndrome characterized by heavy sweating, weakness, dizziness, and nausea, resulting from prolonged heat exposure if the body's water and salt are not replenished.

• Heat Stroke: A life-threatening, extreme condition in which the body's heat regulation mechanism fails, resulting in core body temperatures above 104°F (40°C). It manifests through confusion, loss of consciousness, and possible failure of organs.

Active muscles generate significant heat, most significantly during strenuous exercise, such as firefighting. Excess heat, if in quantities greater than the body's cooling capacity, raises core body temperature, resulting in the possibility of heat illness. [11]

Furthermore, the thermal characteristics of protective clothing also influence heat dissipation. Whereas protective clothing prevents external heat sources from reaching the body, the same clothing also prevents the evaporation of sweat [12], leading to less efficient cooling and possibly aggravating heat stress.

6. Thermal effect on the surroundings of the fire and humans

Fires generate intense heat that impacts the environment and the human body in numerous ways. The thermal energy released during combustion travels through various mechanisms to cause structural damage, environmental harm, and very hazardous health consequences to those exposed to the fire. [13]

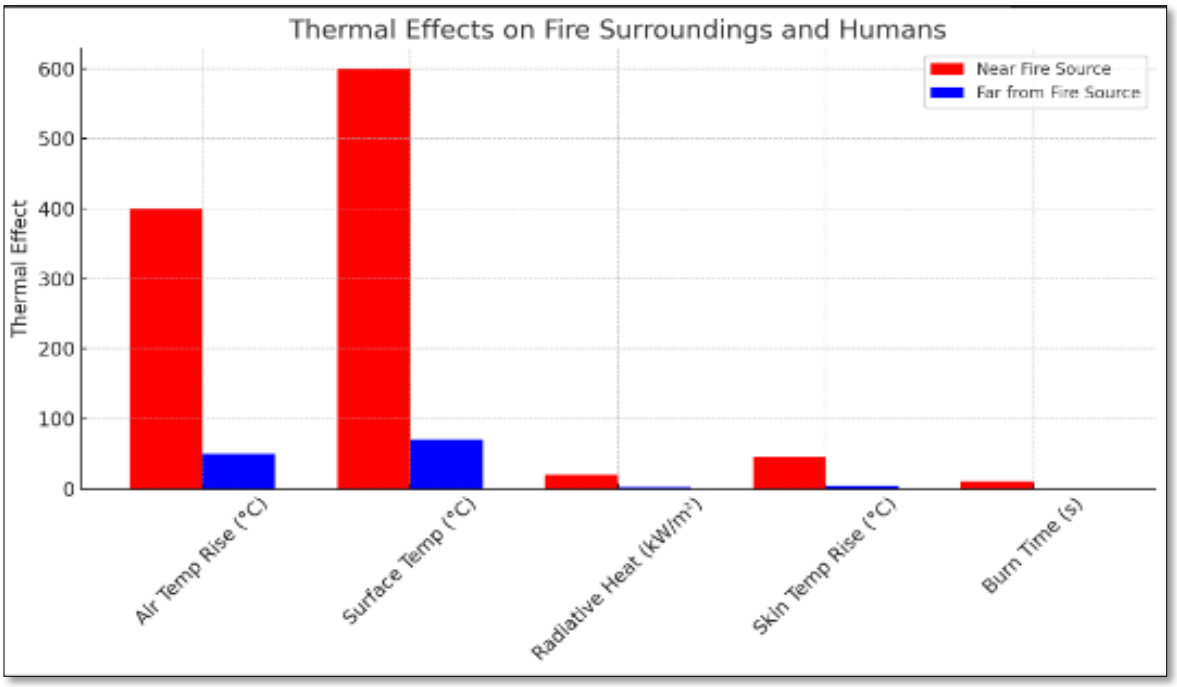

Figure I-4 : histogram visualizing the thermal effects on the surroundings of a fire and on humans. [17]

histogram illustrating the heat effects on the environment of a fire as well as on people. It juxtaposes near-fire conditions with conditions at a distance (in a safety zone):

● Air Temperature Increase and Surface Temperature peak abruptly around burning areas.

● Radiant heat flux can be as high as ~20 kW/m² near fires, which can produce dangerous elevations of skin temperatures with associated burn injuries within less than 10 seconds.

By contrast, the impacts are much reduced within safer areas, demonstrating the role of protection and distance.

5.1. Thermal Impacts on the Environment

5.1.1. Structural Damage

Infrastructure and buildings deteriorate with exposure to intense heat.

Steel weakens between 600-800°C (1112-1472°F), which can result in collapse.

Concrete can explode due to moisture expansion inside. [14]

Glass will break at around 250°C (482°F), affecting visibility and safety. [15]

5.1.2. Environmental Impact

Wildfires alter ecosystems, destroy habitats, and cause long-lasting ecological damage. [16]
Smoke and noxious gases (carbon monoxide, nitrogen oxides) pollute the air, affecting respiratory health.
Temperatures altered by fire can produce local weather conditions, enhance wind, and propagate fire. [17]

5.2. Thermal Effects on the Human Body

When exposed to fire, the human body responds to heat stress in a number of ways, affecting both the skin and internal organs.

5.2.1. Burns and Skin Damage

Temperature (°C/°F) Effects on Human Skin
44°C (111°F): Damage to cells after extended exposure. [18]
55°C (131°F): First-degree burns in 30 seconds.
70°C (158°F):Second-degree burns in 1 second.
160°C (320°F):Instant third-degree burns; damage to nerves.

5.2.2. Heat Stress and Heat Stroke

Prolonged exposure to heat leads to heat exhaustion and heat stroke. Symptoms: Dizziness, dehydration, confusion, rapid heart rate, organ failure. [19] Core temperature above 40°C (104°F) is life-threatening. [20]

5.2.3. Inhalation Injuries

Noxious smoke and hot gases can lead to airway burns and lung damage. Symptoms: Hoarseness, coughing, breathing difficulty. Carbon monoxide (CO) poisoning reduces the supply of oxygen, resulting in suffocation. [21]

7. Burn Types and Their Effects

Burn injuries are categorized based on the depth and severity of tissue damage:

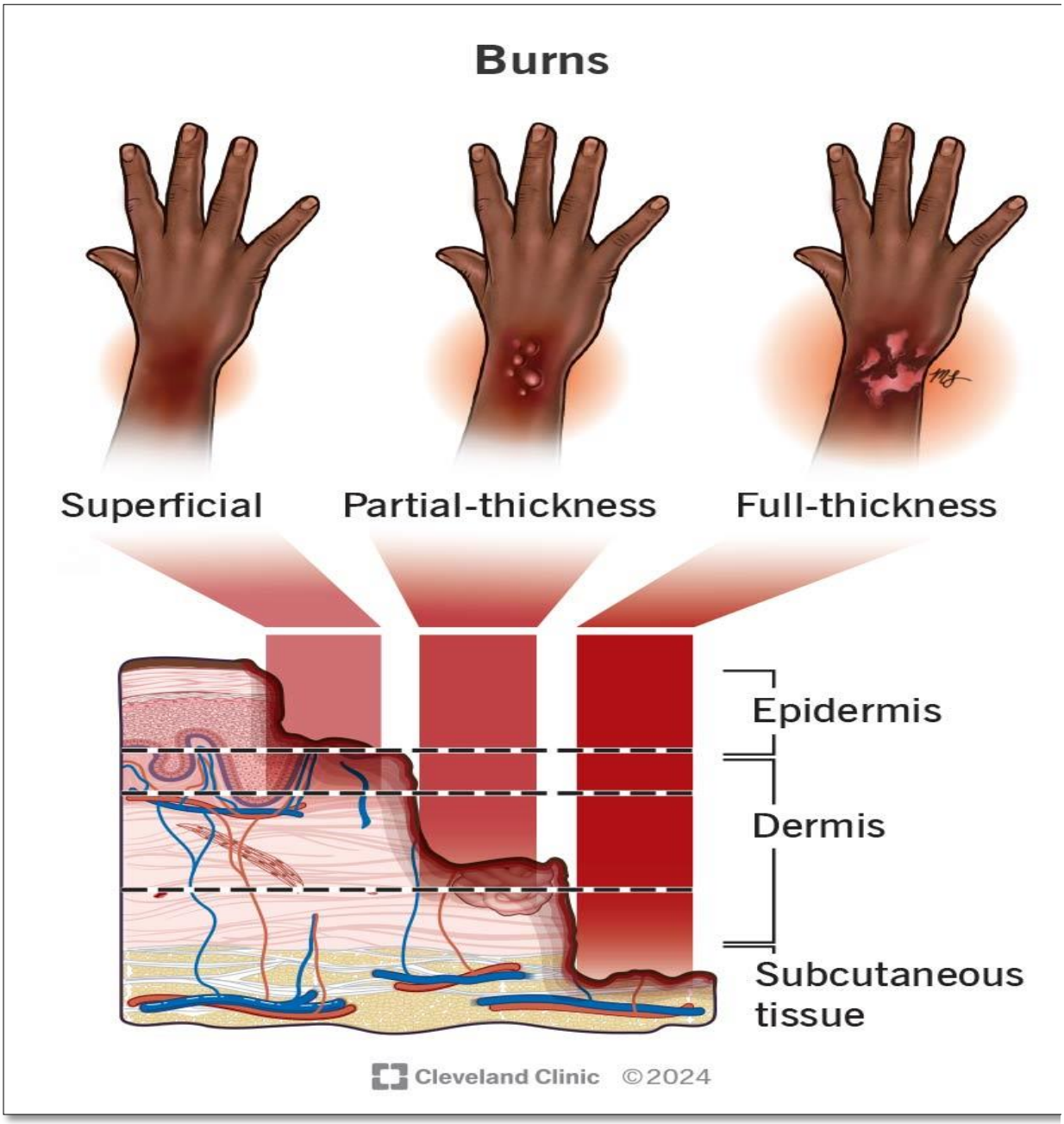

Figure I-5 :Burn Types and Their Effects. [26]

First-Degree Burns (Superficial Burns): These affect only the outer layer of the skin, known as the epidermis. Symptoms include redness, pain, and minor swelling, without blisters. Healing typically occurs within a week without scarring.

Second-Degree Burns (Partial Thickness Burns): These involve both the epidermis and part of the dermis. The burn site appears red, blistered, and may be swollen and painful. Healing can take several weeks and may result in scarring.

Third-Degree Burns (Full Thickness Burns): These extend through the dermis and affect deeper tissues. The burn site may appear white, charred, or leathery, and sensation in the area can be absent due to nerve damage. Such burns often require surgical intervention and can lead to significant scarring and functional impairment.

For firefighters, understanding these burn types is crucial, as their work environment presents constant exposure to burn hazards. Effective protective measures and prompt medical attention are vital to mitigate the adverse effects of burns. [22]

8. Fire Protection Methods

Fire protection encompasses strategies designed to prevent, control, and mitigate fire hazards:

Active Fire Protection: Involves systems that require action to operate, such as fire extinguishers, sprinkler systems, and fire alarms. These systems detect and suppress fires in their early stages, minimizing damage and enhancing safety.

Passive Fire Protection: Utilizes building components to contain fires or slow their spread, including fire-resistant walls, floors, and doors. Materials used in passive protection are designed to withstand high temperatures and prevent structural collapse during a fire. [23]

Firefighter Training and Protocols: Comprehensive training programs equip firefighters with the knowledge and skills to assess risks, execute effective firefighting techniques, and perform rescues safely. Regular drills and adherence to established protocols are essential components of fire protection. [24]

●**Fire Spread Over Time (Line Graph):** Simulates how fire would spread with no protection, passive protection only, and combined active-passive systems. [25]

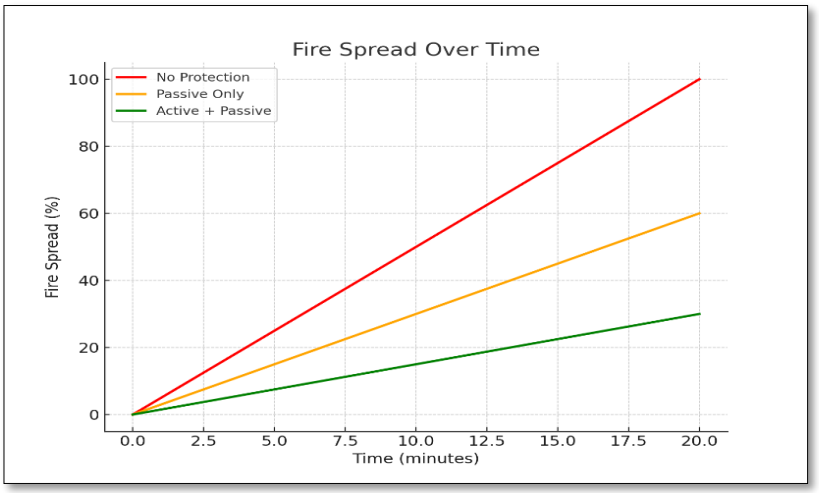

Figure I-6 : Fire Spread Over Time. [31]

●**Fire Protection Strategies (Pie Chart):** Illustrates the general proportion of fire safety investments or strategies in typical fire safety designs. [26]

Figure I-7 : Distribution of Fire Protection Strategies. [33]

9. Firefighter Protective Clothing

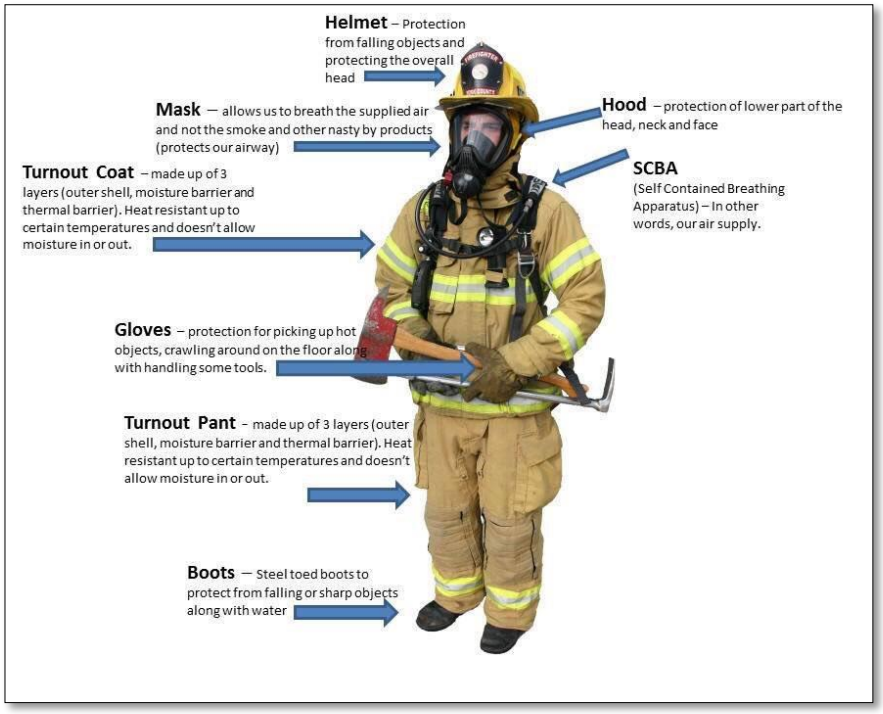

Figure I-8 : : Firefighter equipment. [34]

Protective clothing is a critical element in safeguarding firefighters from thermal hazards:

Global Standards: Internationally, firefighter gear typically consists of multiple layers:

Outer Shell: Provides flame resistance and shields against physical hazards. Materials like Nomex and Kevlar are commonly used for their durability and heat-resistant properties. [27]

Moisture Barrier: Prevents the ingress of water and chemicals while allowing perspiration to escape, maintaining comfort and reducing heat stress. [28]

Thermal Barrier: Insulates against extreme heat, protecting the wearer from high temperatures encountered during firefighting operations. [29]

These layers work in unison to offer comprehensive protection. Advancements in material science have led to the development of fabrics that enhance heat resistance and reduce the overall weight of the gear, improving mobility and comfort.

Firefighter Clothing in Algeria: In Algeria, firefighting services utilize protective clothing that aligns with international standards, incorporating multi-layered ensembles designed for thermal protection. However, challenges such as resource limitations and the need for region-specific adaptations exist. Efforts are ongoing to enhance the performance of firefighting systems, including the adoption of fireproofing measures and the improvement of protective gear to meet the unique demands of the Algerian environment.

10.Conclusion

This chapter has provided a comprehensive overview of the technological aspects related to the thermal hazards encountered in firefighting operations. It examined the classification of fires, the nature of firefighting activities, and the associated exposure risks, highlighting the complex and dangerous environments in which firefighters operate. A thorough understanding of these hazards is essential for developing effective safety strategies and improving operational protocols.

Additionally, the chapter explored the physiological and structural implications of thermal exposure, including the composition of human skin, the body's thermal regulation mechanisms, and the impact of extreme heat on both the environment and human health. The analysis of burn types and their severity further underscores the need for preventive measures and timely medical intervention.

Moreover, the study emphasized the critical role of fire protection systems—both active and passive—in mitigating fire-related risks. The importance of advanced protective clothing was also discussed, with attention to international standards and the specific context of firefighting in Algeria. While significant progress has been made in aligning with global best practices, continued efforts are necessary to enhance protective measures and adapt them to regional requirements.

In summary, this chapter establishes the foundational knowledge required for understanding the thermal risks faced by firefighters and sets the stage for more detailed analysis in subsequent chapters, particularly with regard to thermal modeling and protective equipment performance.

Chapter II

State of the art

II. Chapter 02 : State of the art

1. Introduction

In recent years, research in firefighter protective clothing has accelerated with growing awareness of thermal hazards and their impact. The chapter's goal is to present an integrated view of recent work concerning fire behavior, burn injury processes, and thermal performance of protective garments. The literature is categorized under three focus topics: fire behavior , burn injury processes , and firefighter protective clothing ensembles .

2. Description of Some Current Studies

2.1Fires

2.1.1. Climate Change and Fire Severity

A study published in Nature indicates that climate change is responsible for increasing fire weather days across 76% of the globe's vegetated land area from 1979 to 2019. Global warming has also increased the frequency and severity of wildfires. Lengthening dry seasons and warming climates result in the spread of fire-prone areas. [30]

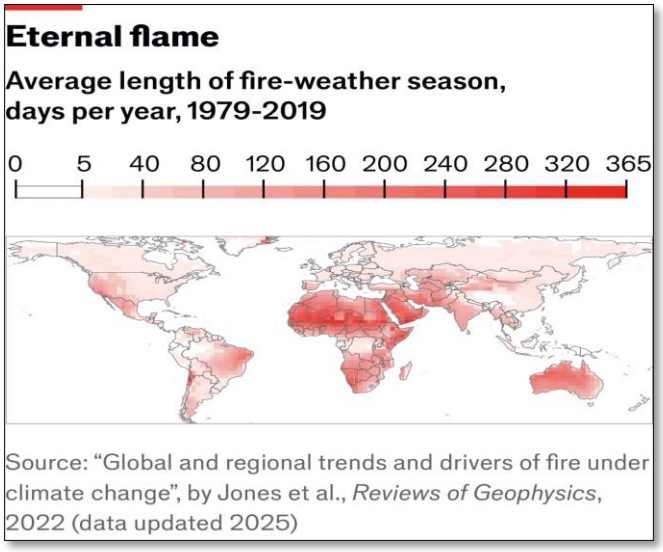

Figure II-1 : Average length of fire-weather season, days per year , 1979-2019. [39]

2.1.2.Experimental Studies on Fire Spread Behavior

In one controlled burn experiment, wind speed alone increased the fire spread rate by up to 300%, even when fuel and humidity were constant. Field and laboratory experiments examine the role of several factors (vegetation type, humidity, wind) in influencing fire spreading. [31]

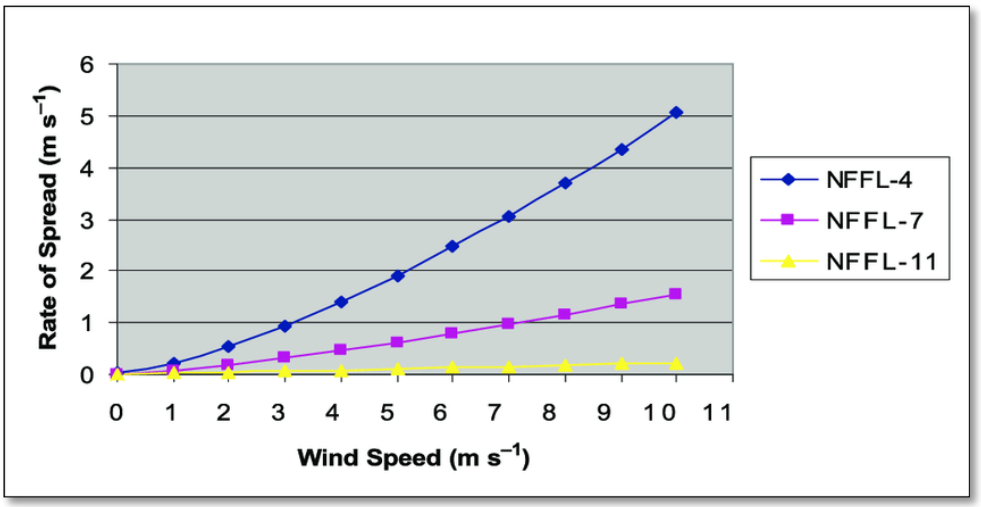

Figure II-2 : Rate of fire spread under extreme wind conditions. [41]

2.2.Burn Injuries

Tissue damage due to thermal energy is the focus of research in this context. Biomedical literature clearly defines thresholds for first-, second-, and third-degree burns.

2.2.1.Burn Injury Patterns Among Firefighters

An extensive study done in Korea investigated burn injuries in 536 active firefighters:

- Incidence of burns: 22% reported burns
- Severity: The burns involved in 93% of cases covered less than 1% of total body area.
- Common locations: Hands (37%) and head/neck (34%) were affected most often. [32]

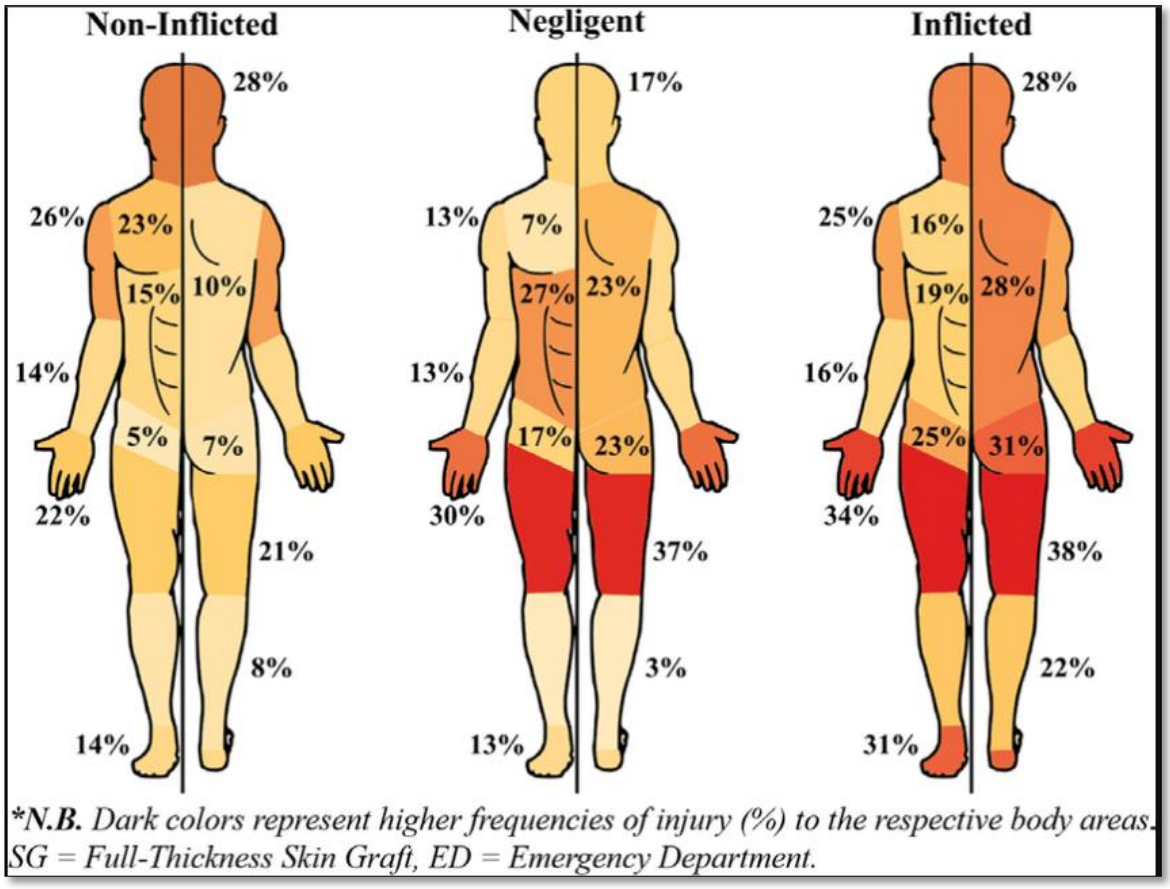

Figure II-3 : Burn Distribution. [43]

2.2.2.Factors Influencing Burn Injuries

Studies have shown that numerous factors are responsible for both the incidence and degree of burn injuries:

-Heat Source Characteristics: The type and intensity of heat exposure.

-Protective attire: Composition and structure of firefighter protective equipment.

-Air Gaps: Thickness and characteristics of air films in between skin and clothing.

These variables control the heat transfer to the skin internally, and impact risk of burning. Predictive models have now been formulated to estimate exposure time and distance safely. [33]

2.3.Firefighter Protective Clothing

Wildland fire-fighting is physically strenuous work conducted in hot environments. [34] Personal protective clothing (PPC) is vital for thermal protection but has the potential to increase

physiological load and decrease performance. This research compared how four types of PPC impact the physiological responses of firefighters in moderate heat (30°C, 30% RH). Eight healthy fire-fighters conducted a walking trial in standard sportswear and in four sets of PPC constructed from different materials (viscose, Nomex, Kevlar, P-140, and fire-resistant cotton). They wore a 20 kg load in order to mimic actual conditions [35]. Measurements were taken of heart rate, respiratory gases, gastrointestinal temperature, lactate in the blood, perceived effort, and temperature and humidity in the PPC. Heat balance indices were also determined. Generally, physiological load was not significantly increased by the use of PPC. Nevertheless, factors such as inner humidity, retention of sweat, dry heat exchange, and insulation by the fabric were influenced by fabric composition. These observations emphasize the importance of fabric selection in enhancing moisture control and firefighter protection in the vicinity of fire.

Participants involved in the study are eight healthy, active male wildland firefighters (average age 30.8 ± 8.4 years, height 1.79 ± 0.06 m, weight 76.9 ± 10.8 kg, VO_2max 55.4 ± 9.1 $ml \cdot kg^{-1} \cdot min^{-1}$, body surface area 1.9 ± 0.2 m^2) took part in this study. They regularly performed endurance training (45–60 minutes, three times per week). All participants gave written informed consent. The study followed the ethical standards of the Helsinki Declaration and was approved by the Ethics Committee of the University of León, Spain.

As experimental Design , each participant completed six testing sessions, spaced at least 48 hours apart. The first session involved a maximal exercise test (Bruce protocol) [36] to assess fitness. In the remaining five sessions, participants performed a 120-minute submaximal walking test wearing either standard sportswear or one of four different PPC types, following a balanced Latin Square design. All PPC met ISO (2003) [37] standards and are used by Spanish wildland firefighters. Only basic underclothing (cotton t-shirt, underwear, and socks) was worn underneath, and accessories like helmets, gloves, goggles, and boots were excluded. Garment details are listed in Table 1. To simulate real firefighting, participants carried a 20 kg backpack pump during each test and wore the same running shoes (250–300 g per shoe).

Table II-1 : Personal Protective Clothing (PPC) Characteristics. [49]

Layer	PPC#1 Single	PPC#2 Reflective double layer on shoulders	PPC#3 Single	PPC#4 Single
Composition				
FR viscose (%)	65	65	56	
Nomex (%)	30	30	34	
Kevlar (%)	5	5	8	
P-140 (%)			2	
FR cotton (%)				100
Mass (g)	1,460	1,560	1,440	1,000
Surface mass ($g \cdot m^{-2}$)	270	270	225	310
Total mass (kg)*	79.6 ± 7.4	79.5 ± 6.6	79.7 ± 7.0	78.1 ± 6.5
Fabric thermal resistance ($m^2 \cdot K \cdot W^{-1}$)	0.0192	0.0192	0.0213	0.0260
Fabric evaporative resistance ($m^2 \cdot Pa \cdot W^{-1}$)	3.79	3.79	3.45	3.51

With FR: Fire Resistant

*Subjects' mass while wearing the PPC.

The testing protocol was as follow : All the tests were done using a treadmill (h/p/cosmos pulsar, h/p/cosmos sports and medical GmbH, Nussdorf-Traunstein, Germany). A 10 min warm-up at 60% maximum heart rate (8–10 km·h−1), followed by 5 min of stretching, preceded each test. The maximal test was conducted according to the protocol set out by Bruce (1971) [38]. A speed of 2.5 km·h−1 and 10% grade were used to initiate the test. Speed and grade were raised every 3 min to volitional fatigue.

The submaximal tests were conducted at the same time of the day (12:00 to 16:00 h) in a climate-controlled environment within a laboratory at 30°C of air temperature and 30% relative humidity, simulating the conditions analyzed in real wildland fires (Rodríguez-Marroyo et al., 2012) [39]. Each protocol consisted of 6 walking sets at 6 km·h−1 and 1% of slope with 5 min of passive rest periods in between. Each set lasted 15 min, although the first set lasted 20 min, thereby the total length of the test was 120 min. At recovery times, 0.15 ml·kg−1 of water every 1 min of exercise at 15°C was provided to avoid that dehydration of subjects restricted the sweat rate (Cheuvront et al., 2010) [40]. This protocol was adopted from previous studies (Selkirk and McLellan, 2004) [41], and the adopted speed enabled subjects to execute an exercise intensity from 60 to 70% of the maximal heart rate, simulating the working condition of wildland firefighters (Rodríguez-Marroyo et al., 2012) [42].

As results, there was no significant interaction between the type of clothing worn and the duration of the trials for most physiological responses, including oxygen uptake (VO_2), ventilation, heart rate, blood lactate, gastrointestinal temperature, physiological strain index (PSI), the temperature underneath the protective clothing, and perceived exertion (RPE), as shown in Figure 12.

The average values recorded across all trials were as follows:

VO_2: 1.5 ± 0.3 L/min

Ventilation: 48.4 ± 8.5 L/min

Heart Rate: 114 ± 15 bpm

Blood Lactate: 1.5 ± 0.2 mmol/L

Gastrointestinal Temperature: 37.4 ± 0.5°C

PSI: 3.2 ± 0.7

Temperature under the protective clothing: 32.7 ± 1.2°C

RPE: 10.7 ± 2.0

Similarly, no significant effects of time alone were observed on these parameters.

However, a notable exception was found in the increase of gastrointestinal temperature. Participants wearing PPC#3 experienced a significantly greater rise in core temperature (0.7 ± 0.3°C) compared to those wearing the other protective clothing configurations (PPC#1, PPC#2, and PPC#4 showed increases of just 0.2 ± 0.3°C, 0.2 ± 0.5°C, and 0.2 ± 0.3°C, respectively) and sportswear (0.3 ± 0.3°C).

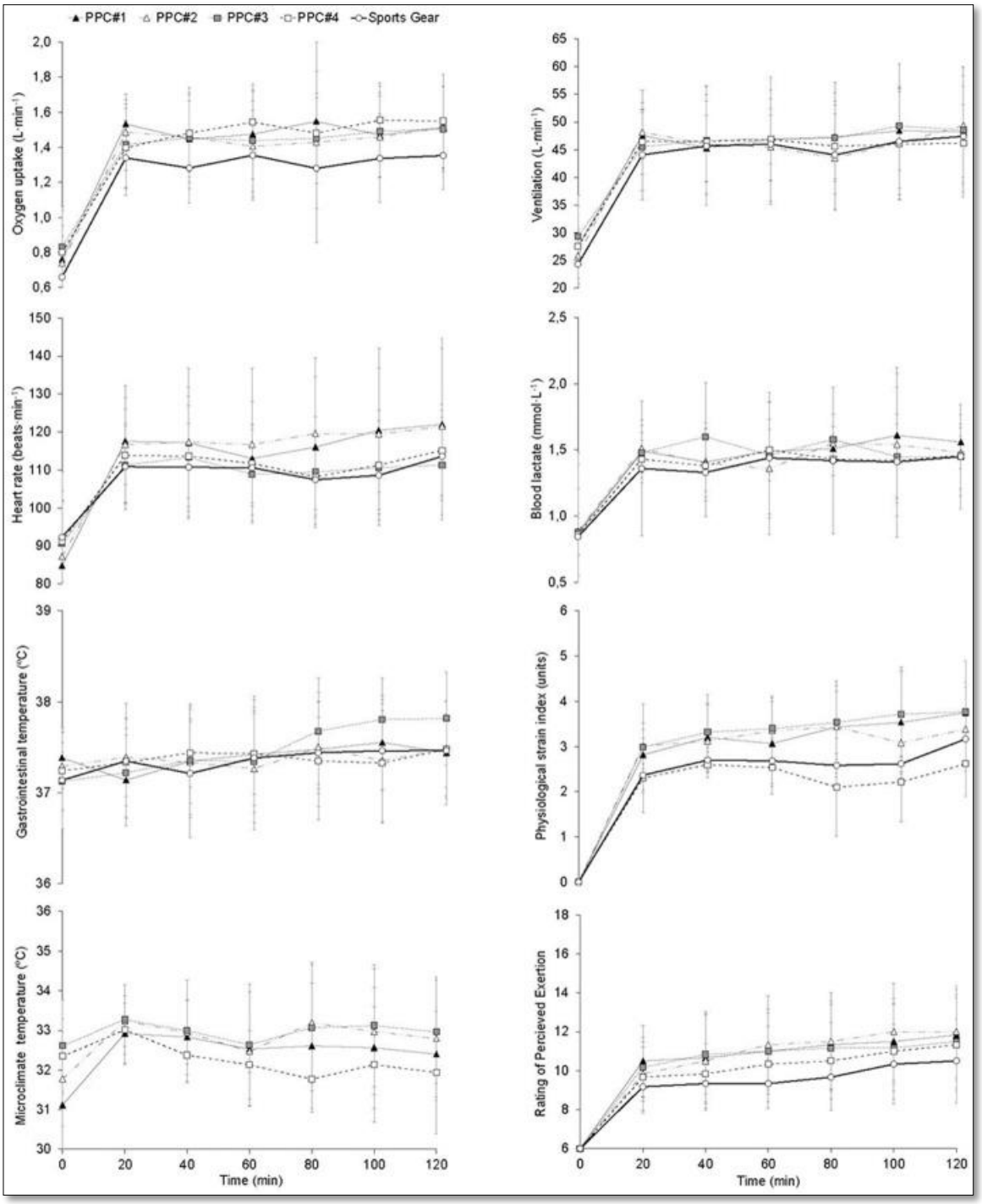

Figure II-4 : Comparative responses of oxygen uptake, ventilation, heart rate, blood lactate concentration, gastrointestinal temperature, physiological strain index, temperature of the microclimate underneath the personal protective clothing (PPC), and rating of perceived exertion during the different trials. [43]

Relative Humidity Results was as follow : the microclimate under the protective clothing (PPC) showed significantly higher relative humidity levels in PPC#2 and PPC#3 compared to PPC#4 (81.2 ± 4.7% and 77.7 ± 5.0% vs. 71.7 ± 4.9%, respectively; $p < 0.05$). From the 60-minute mark onward, PPC#4 consistently showed the lowest humidity levels among all configurations (Figure 13).

Overall, humidity levels rose more rapidly during the first hour of the trials (0–60 minutes), then increased more gradually during the second hour (60–120 minutes), as shown in Figure 2. When comparing the early phase (5–20 minutes) to the later phase (60–120 minutes), the relative humidity increased significantly—from around 63% to approximately 84% ($p < 0.05$).

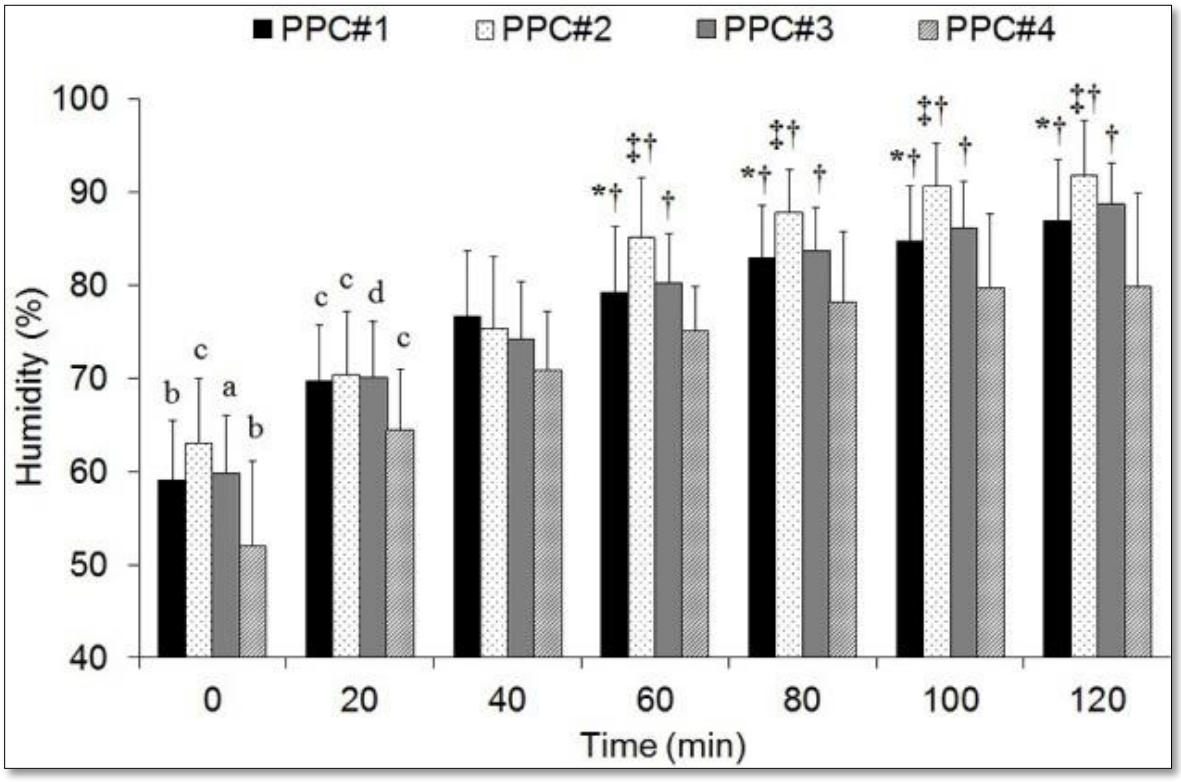

Figure II-5 : Relative humidity pattern recorded during the trials performed with the different personal protective clothing (PPC).

*Differences with PPC#2 ($p < 0.05$).

‡Differences with PPC#3 ($p < 0.05$).

†Differences with PPC#4 ($p < 0.05$).

aDifferences with 20–120 min ($p < 0.05$).

[b]Differences with 40–120 min ($p < 0.05$).

[c]Differences with 60–120 min ($p < 0.05$).

[d]Differences with 100–120 min ($p < 0.05$). [44]

Sweat Production and Comfort Results was as follow : Total sweat production was similar across all types of protective clothing (PPC) and when participants wore sports gear (Table 2). Likewise, the amount of sweat absorbed by the underwear did not vary significantly between the different trials.

However, PPC#1 stood out with the lowest amount of sweat residue retained within the suit ($p < 0.05$), which translated into the highest sweat evaporation efficiency compared to the other PPCs tested ($p < 0.05$). This means PPC#1 was more effective in allowing sweat to evaporate rather than accumulate inside the suit.

Participants also reported a lower sensation of wetness when wearing PPC#1, scoring 5.6 ± 0.3 on the moisture sensation scale, which was significantly lower than the scores for PPC#2 (7.6 ± 0.9), PPC#3 (7.0 ± 0.6), and PPC#4 (8.2 ± 0.5) ($p < 0.05$). The driest and most comfortable feeling was reported when wearing the sports gear, which scored the lowest at 3.8 ± 1.0.

Table II-2 : Sweat Measurements Analyzed in This Study (mean ± SD) [57]

	PPC#1	PPC#2	PPC#3	PPC#4	Sports gear
Total sweat production (g)	1,910 ± 360	2,342 ± 450	2,110 ± 390	1,968 ± 370	1,925 ± 447
Sweat residue in underwear (g)	367 ± 53	368 ± 70	361 ± 54	409 ± 61	335 ± 156
Sweat residue in garment (g)	178 ± 51‡†	579 ± 278	545 ± 156	418 ± 124	
Sweat evaporation (g)	1,514 ± 327	1,395 ± 161	1,274 ± 268	1,189 ± 338§	1,609 ± 251
Sweat efficiency (%)	74 ± 5‡†§	61 ± 7§	59 ± 5§	58 ± 9	84 ± 8

With : PPC, personal protective clothing.

*Differences with PPC#2 ($p < 0.05$).

‡Differences with PPC#3 ($p < 0.05$).

†Differences with PPC#4 ($p < 0.05$).

$Differences with Sports Gear ($p < 0.05$).

According to heat balance results the estimated heat balance parameters are presented in Table 3. Dry heat exchange was significantly different in PPC#2 and PPC#3 compared to PPC#4 ($p < 0.05$), indicating that these suits managed heat transfer differently. Additionally, PPC#1 had the lowest total clothing insulation among all the configurations tested ($p < 0.05$), suggesting it provided better heat dissipation and less thermal resistance.

Table II-3 : Estimated Parameters of Heat Balance Analysis (mean ± SD) [58]

	PPC#1	PPC#2	PPC#3	PPC#4
Heat storage ($W \cdot m^{-2}$)	4.5 ± 7.5	5.5 ± 14.0	8.1 ± 6.3	3.8 ± 6.0
Metabolic heat production ($W \cdot m^{-2}$)	250.5 ± 23.7	238.4 ± 26.1	243.2 ± 34.9	248.1 ± 22.4
Respiratory heat exchange ($W \cdot m^{-2}$)	10.2 ± 1.0	9.7 ± 1.0	9.9 ± 0.9	10.1 ± 0.9
Evaporative heat loss from skin ($W \cdot m^{-2}$)	251.5 ± 48.1	232.9 ± 30.5	210.9 ± 42.9	197.4 ± 57.7
Dry heat exchange ($W \cdot m^{-2}$)	15.8 ± 15.7	9.9 ± 12.4†	11.4 ± 6.7†	30.4 ± 24.1
Total clothing insulation ($m^2 \cdot °C \cdot W^{-1}$)	0.08 ± 0.06‡‡	0.35 ± 0.38	0.31 ± 0.22	0.26 ± 0.36

With : PPC, personal protective clothing.

*Differences with PPC#2 ($p < 0.05$).

‡Differences with PPC#3 ($p < 0.05$).

†Differences with PPC#4 ($p < 0.05$).

As a Discussion we can say this study aimed to examine how different types of protective clothing (PPC) affect the physiological strain experienced by wildland firefighters. Contrary to our expectations, we did not observe significant differences in cardiorespiratory responses—such as heart rate, oxygen consumption (VO_2), or ventilation—between the clothing ensembles (Figure 1).

This contrasts with earlier studies that reported increases of 10–20% in physiological strain with different PPC types (Baker et al., 2000 [45]; Dorman & Havenith, 2009 [46]; Wen et al., 2015 [47]). Even greater effects (over 20%) have been observed in structural firefighters, particularly when wearing self-contained breathing apparatus due to the added weight of 10–20 kg (Taylor et al., 2012 [48]; Lee et al., 2014 [49]).

In our study, the average increase in physiological strain when wearing PPC was about 12%. This lower impact may be explained by the reduced thermal insulation of the PPCs used by wildland firefighters (~0.23 $m^2 \cdot K \cdot W^{-1}$) compared to those worn by structural firefighters (~0.47 $m^2 \cdot K \cdot W^{-1}$) (Raimundo & Figueiredo, 2009 [50]; Holmér et al., 2006 [51]), which likely allowed for greater heat dissipation. Additionally, our participants completed the trials without gloves, helmets, or boots, increasing exposed skin surface and enhancing heat loss (Holmér, 2006 [52]; Lee et al., 2014 [53]). In line with this, Lee et al. (2014) found no significant differences in VO_2 or heart rate when firefighters performed similar tests without this additional gear.

The limited weight differences between clothing configurations may also have contributed to the uniformity of physiological responses. Previous studies noted that over half of the rise in metabolic rate is due to the weight of PPC alone (Dorman & Havenith, 2009 [54]). Consistently, no significant differences in cardiorespiratory metrics or perceived exertion (RPE) were observed when wearing lightweight workwear versus standard sportswear (Kofler et al., 2015 [55]).

Another key factor could be the high aerobic fitness of our participants. Their average VO_2max was approximately 28% higher than previously reported values for wildland firefighters (~43 $ml \cdot kg^{-1} \cdot min^{-1}$) (Phillips et al., 2011 [56]). Greater fitness levels are associated with improved tolerance to physical effort in hot conditions and reduced physiological strain while wearing PPC (Selkirk & McLellan, 2001 [57]).

Although wearing PPC in hot environments is typically linked to an increase in core body temperature (Smith & Petruzzello, 1998 [58]; Bruce-Low et al., 2007 [59]), we did not detect any significant differences in gastrointestinal temperature in our moderate environmental conditions. Even though PPC#3 did lead to a greater increase, all recorded temperatures stayed below 38°C, a level generally considered the threshold for impaired performance under heat stress (Gonzalez-Alonso et al., 1999 [60]). It's possible that cardiovascular adjustments—such as increased heart

rate and cutaneous blood flow—helped stabilize core temperature. This is supported by our finding that heart rate was ~5% higher on average when wearing PPC, likely reflecting increased skin blood circulation to facilitate heat dissipation (Cheuvront et al., 2010 [61]). The oxygen uptake (VO_2) was also slightly (~200 $ml \cdot min^{-1}$) higher with PPC, though not statistically significant (Figure 1), possibly due to the metabolic cost of carrying additional clothing weight (Dorman & Havenith, 2009 [62]).

We observed a consistent temperature gap of around 2.5°C between the microclimate inside the PPC and the ambient environment. Interestingly, PPC#2 and PPC#3 recorded higher internal temperatures (by ~0.8°C) than the other garments, particularly after the first hour of exercise (Figure 1). This may be due to reduced dry heat exchange, likely influenced by the clothing's material properties such as fabric thickness and air permeability (Havenith et al., 2011 [63]). While all PPCs used heat-resistant fabrics like Nomex and Kevlar blended with fire-resistant viscose, PPC#3 had 10% less viscose, possibly lowering its air permeability and heat dissipation. Similarly, PPC#2 had an extra fabric layer over the shoulders, increasing its insulation and restricting heat loss (Holmér, 2006 [64]).

Although no significant differences in evaporative heat transfer were found between the clothing types (Table 3), this may reflect measurement variability. Still, the higher relative humidity levels observed under PPC#2 and PPC#3 suggest reduced sweat evaporation, which aligns with previous studies linking elevated humidity in the microclimate to impaired evaporative cooling (Kwon et al., 1998 [65]; Yoo & Barker, 2005 [66]; Bröde et al., 2008 [67]).

Even though PPC#4 had the lowest relative humidity (Figure 2), it did not result in improved sweat evaporation. In fact, it retained the most sweat and showed a sweat efficiency comparable to PPC#2 and PPC#3 (~60%) (Table 2). This could be attributed to its 100% cotton composition and greater thickness. Cotton is known for its high moisture retention and relatively low efficiency in promoting evaporation when sweating is intense (Kwon et al., 1998 [68]). These findings support earlier research (Holmér, 1985 [69]), which highlights the superior moisture management capabilities of synthetic fibers like polyester, nylon, and aramid.

While higher sweat retention might improve thermal conductivity and reduce heat strain during moderate activity (Chen et al., 2003 [70]; Keiser & Rossi, 2008 [71]), it can become a liability in

real wildfire conditions. In such scenarios, wildland firefighters are exposed to both radiant and convective heat, with heat fluxes ranging from 0.42 to 8.37 $kW \cdot m^{-2}$ (Mäkinen, 2005 [72]). Under these conditions, moisture retained in clothing could reverse the heat transfer process, increasing the risk of burns rather than providing protection (Holmér, 2006 [73]; Keiser & Rossi, 2008 [74]).

From this perspective, PPC#1 appears to offer the best performance. It retained approximately 65% less moisture than the other suits (Table 2), provided the highest sweat evaporation efficiency, and resulted in the lowest reported sensation of wetness—key indicators of comfort and thermoregulatory efficiency. This could play a significant role in enhancing firefighters' operational performance and safety during wildfire suppression efforts (Nayak et al., 2014 [75]).

The resulting conclusion was like follow : although no significant differences were found in core cardiorespiratory or thermoregulatory responses (such as heart rate, VO_2, blood lactate, PSI, or gastrointestinal temperature) between the PPC configurations, the materials and design of the clothing clearly influenced moisture management and wearer comfort. PPC#1 provided the best balance, demonstrating superior sweat evaporation, lower moisture retention, and higher subjective comfort. These features may contribute to greater protection and improved performance for wildland firefighters in real-world scenarios.

3. Experiments and Numerical Studies

To evaluate the thermal protection offered by firefighter clothing, both experimental setups and numerical simulations are employed. These approaches aim to analyze heat transfer through multilayer protective systems under various fire conditions. Among numerical tools, MATLAB and console-based modeling environments have become standard due to their efficiency and flexibility in solving heat transfer equations.

3.1.Experimental Studies

Experimental methods are crucial for validating theoretical models. These include:

Cone calorimeter tests: Used to study flammability, ignition time, and heat release rate of textiles.

Thermal manikins: Measure temperature profiles across clothing layers simulating human skin.

Guarded hot plates: Evaluate thermal resistance and conductivity of multi-layered fabrics.

Example: In a full-scale fire exposure test, thermal manikins wearing three-layer turnout gear recorded heat fluxes over 10 kW/m². The data helped calibrate numerical models for injury prediction.

3.2.Numerical Studies

A. One-Dimensional Heat Transfer Models in MATLAB

MATLAB is widely used to simulate transient heat transfer in multilayer systems such as firefighter clothing. A typical model includes:

Discretization of each fabric and skin layer.

Application of boundary conditions (heat flux, temperature).

Solving heat conduction equations using Finite Difference Method (FDM) or Runge-Kutta schemes.

In a MATLAB-based study by Mandal et al. (2020), a one-dimensional model simulated the temperature rise across four layers (outer shell, moisture barrier, thermal liner, and skin simulant) over 180 seconds. Results predicted 2nd-degree burn thresholds at the skin layer when outer heat flux exceeded 8.5 kW/m².

In their pivotal work titled "A Model of Heat Transfer in Firefighting Protective Clothing During Compression After Radiant Heat Exposure", Su et al. (2016) [76] present a comprehensive numerical model designed to predict the thermal responses of multi-layer firefighter protective clothing subjected to combined thermal and mechanical stress. The study addresses a significant gap in the literature by simulating heat transfer behavior not only under radiant heat exposure but also under subsequent compression—a common real-life condition when firefighters come into contact with hot surfaces during operations.

The proposed model is based on a one-dimensional, transient heat transfer approach that incorporates multiple fabric layers (outer shell, moisture barrier, and thermal liner), an intermediate air gap, and underlying skin tissue layers (epidermis, dermis, and subcutaneous tissue). It accounts for both radiative and conductive heat transfer mechanisms. The model is unique in its consideration of dynamic fabric compression, where changes in fabric thickness and air content are introduced based on applied contact pressures. This allows the simulation to reflect more accurately the real thermal risks faced by firefighters in the field.

For numerical implementation, the authors employed a finite difference method using the Crank–Nicholson implicit scheme, and all simulations were executed using MATLAB (version 8.3). The model was validated experimentally using a Sensor Evaluation Tester (SET) apparatus, in accordance with ASTM F2731. Tests involved subjecting fabric systems to 8.5 kW/m² radiant heat flux for 300 seconds, followed by a 13.8 kPa compression phase lasting an additional 600 seconds. The experimental results, particularly the recorded temperatures at the epidermis–dermis interface and times to second- and third-degree burns, showed strong correlation with the simulation outcomes, confirming the model’s validity and predictive accuracy.

A key contribution of the study lies in its parametric analysis, which explored the effects of varying contact pressures, temperatures, and air gap sizes. Results showed that:

- Increased contact pressure and temperature significantly reduce the time to burn injuries.
- Air gap thickness, while influential during radiant heat exposure, has a diminished effect once compression occurs.
- Fabric thickness and thermal conductivity are major determinants of thermal protective performance.
- The combined effect of compression and stored thermal energy within the clothing layers intensifies the risk of skin burns.

Overall, the study by Su et al. provides an advanced predictive framework for evaluating the thermal protective performance of firefighting clothing systems under realistic fireground scenarios. The integration of experimental validation and detailed simulation makes this model a valuable tool for material engineering, clothing system design, and fire safety research. It also lays the groundwork for further exploration into more complex geometries, multidimensional heat transfer, and moisture effects.

B. Comsole-Based Simulation Models

The objective of this research is to develop a mathematical model that describes heat transfer within protective clothing systems exposed to routine fire environments, specifically under low levels of radiant heat flux. The aim is to provide a systematic foundation for the engineering of materials and garments that optimize both thermal protection and wearer comfort.

In the initial phase, the study concentrates on formulating a heat transfer model capable of accurately predicting temperature distribution and heat flux within firefighter protective clothing. This model is implemented using the COMSOL Multiphysics® software, which is based on the finite element method. The computational simulations illustrate the temporal evolution of temperature at the inner surface of the protective clothing during exposure to low-intensity radiant heat, as well as throughout the subsequent cooling period. The numerical predictions demonstrated strong agreement with experimental temperature measurements, thereby validating the model's reliability.

In the second phase, the heat transfer model for the multilayer protective garment is extended to include the thermal response of human skin, enabling the prediction of burn injuries. The Pennes bioheat equation is employed to simulate heat transfer within living tissue, and the Henriques burn integral is applied to estimate the duration of exposure that leads to first- and second-degree burns. The results indicate that, even under relatively low radiant heat flux conditions, a standard three-layer thermal protective clothing system is essential to prevent burn injuries and ensure sufficient thermal protection for the wearer. [77]

As methodology the fabrics chosen for the experimental study are widely recognized as high-performance materials commonly employed in the design of thermal protective clothing. The multilayer protective system under investigation is composed of three distinct fabric layers: an outer shell, a thermal liner, and a moisture barrier.

The fundamental physical and thermal properties of each individual (monolayer) fabric are summarized in Table 1.

Table II-4 : Physical and thermal properties of monolayers. [91]

Property	Outer shell	Thermal liner	Moisture barrier
Fabric type	Woven	Nonwoven	Knitted (coated)
Composition	100% Aramid	100% Aramid	Polyurethane coated 100% Aramid
Thickness (mm)	0.5 ± 0.01	1.46 ± 0.03	0.47 ± 0.00
Surface weight (g/m2)	242 ± 2	98 ± 2	195 ± 2
Density (kg/m3)	489 ± 5	67 ± 2	418 ± 6
Thermal conductivity (W/m K)	0.1154 ± 0.0018	0.0633 ± 0.0015	0.0900 ± 0.0001
Thermal diffusivity (mm2/s)	0.248 ± 0.013	0.449 ± 0.001	0.213 ± 0.000
Specific heat capacity (J/kg K)	951 ± 44	2113 ± 89	1011 ± 3

The thickness of each fabric monolayer was measured under a pressure of 1 ± 0.01 kPa in accordance with ISO 5084:1996. Fabric density was calculated based on the measured thickness and the surface mass per unit area, the latter determined using an analytical balance. For each property, the average value was obtained from ten individual measurements to ensure reliability and consistency.

Thermal properties of the fabric samples were evaluated using the Hot Disk TPS 2500 S instrument, following the procedures outlined in ISO 22007-2:2008 [78]. Three independent measurements were conducted for each monolayer, and the average of these values was used for subsequent analysis.

For the purpose of model simplification, all textile layers were assumed to be homogeneous in structure and properties.

Given the relatively small thickness of the protective clothing layers compared to their surface area, a one-dimensional heat transfer model—along the direction normal to the fabric surface—is adopted as a valid simplification. In developing the numerical model, temperature is assumed to vary only with time and spatial position in the thickness direction, denoted as T(t, x).

Heat transfer within the fabric structure is modeled by considering both heat conduction and radiative penetration through the solid phase. Radiative heat transfer is incorporated into the energy equation via a source term, consistent with the approach used in Torvi's model [79]. It is assumed that radiation penetrates only the outermost fabric layer. Additionally, both conduction and radiative heat transfer mechanisms are considered across the air gap separating the fabric and the underlying surface.

Heat conduction is also accounted for through the copper plate and the insulation board, while external convective air flow is neglected. Evaporative heat loss is not included in the current model, as the effects of sweating are not considered. Since all fabric structures employed in this study are composed of aramid fibers—which exhibit low moisture regain (approximately 3–4%)—the associated heat of evaporation is minimal and deemed negligible.

Experimental measurements of the water evaporation rate from the fibers yielded a value of 0.0025 g/m²·s. When multiplied by the latent heat of evaporation of water, this corresponds to a

total energy loss of approximately 5.6 W/m², which is negligible relative to the magnitude of the incident heat flux.

The thermophysical and geometrical properties of human skin used in the model are presented in Table 2.

Table II-5 : Thermophysical and Geometrical Properties of Human Skin. [94]

	Property	Value
Epidermis	Thermal conductivity (W/m·K)	0.255
	Density (kg/m³)	1200
	Specific heat (J/kg·K)	3598
	Thickness (m)	8×10^{-5}
Dermis	Thermal conductivity (W/m·K)	0.523
	Density (kg/m³)	1200
	Specific heat (J/kg·K)	3222
	Thickness (m)	2×10^{-3}
Subcutaneous	Thermal conductivity (W/m·K)	0.167
	Density (kg/m³)	1000
	Specific heat (J/kg·K)	2760
	Thickness (m)	1×10^{-2}
Blood	Density (kg/m³)	1060
	Specific heat (J/kg·K)	3770
	Blood perfusion rate (s^{-1})	1.25×10^{-3}

As Experimental setup to simulate low-level radiant thermal hazards under controlled laboratory conditions, six silicon carbide heating rods were employed as the radiant heat source, in accordance with the NF EN ISO 6942:2002 standard, which specifies procedures for evaluating radiant heat resistance. According to this standard, the incident heat flux density may be selected from predefined levels: 5 and 10 kW/m² (low), 20 and 40 kW/m² (medium), and 80 kW/m² (high), although other values are permissible depending on experimental requirements [80].

In this study, a copper plate calorimeter was used to measure temperature variations. Data acquisition was performed using a computer-based TESTPOINT software system connected to the

calorimeter. The calorimeter itself consisted of a rectangular copper sheet (50 mm × 50.3 mm), 1.6 mm thick, curved longitudinally to a radius of 130 mm and weighing 36 g. A copper-constantan thermocouple was affixed to the rear surface of the plate. Behind the calorimeter, a 9 mm air gap and a 14 mm asbestos-free, non-combustible insulation board were installed.

The test specimens measured 230 mm × 80 mm and were configured to replicate the actual layering of protective clothing systems. Each specimen was secured to a holder using clamps, with a uniform tensioning force of 2 N applied to ensure consistent assembly across all fabric layers.

The radiant source was adjusted to deliver a heat flux of 1000 W/m². Calibration of the heat flux was carried out in strict accordance with NF EN ISO 6942, and the target value was validated using a CAPTEC ultrathin heat flow meter (50 mm × 50 mm). During the experiments, specimens were exposed to radiant heat for a period of 40 minutes. A protective shutter, positioned between the heat source and the specimen, was used to prevent premature exposure and to precisely control the duration of exposure. After the exposure phase, the shutter was closed to initiate the cooling-down period.

Importantly, only the apparatus and calibration methods prescribed in NF EN ISO 6942 were employed. For model validation purposes, only the temperature recorded by the calorimeter was utilized, as the instrument does not introduce significant measurement error. Experiments were conducted under both transient and steady-state conditions. Three specimens were tested, and the average temperature measured by the calorimeter was used in the final analysis.

Figure 4 presents the temporal evolution of temperature as obtained from both experimental measurements and numerical simulation. At the onset of exposure to radiant heat flux ($t = 0$), the calorimeter temperature increases rapidly, reflecting the immediate thermal response of the fabric system. This is followed by a more gradual rise until thermal stabilization is achieved. Upon termination of the radiant heat exposure at $t \geq 2400$ seconds, the temperature begins to decline, eventually returning to the ambient environmental level.

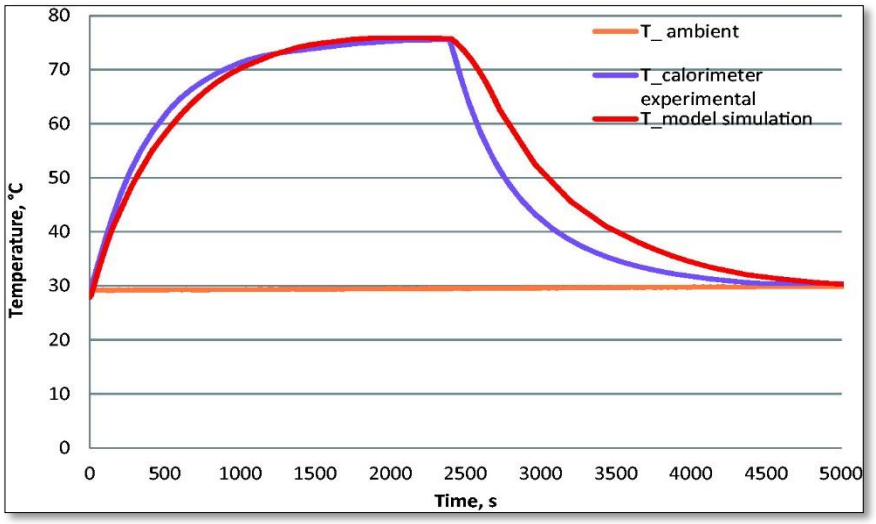

Figure II-6 :Comparison of computational and experimental results of calorimeter temperature for a three-layer system and 1000 W/m2 inward heat flux.

The numerically predicted temperature profiles exhibit good agreement with the experimental data. During the heating phase, the observed discrepancies between simulated and measured temperatures can be attributed to heat accumulation in front of the protective shutter. When the shutter is opened, this accumulated heat is released in addition to the imposed radiative flux, resulting in a steeper initial temperature rise than that predicted by the model. During the cooling phase, the divergence between experimental and numerical results is primarily due to the cooling mechanism associated with the shutter system, which accelerates heat dissipation but was not incorporated into the numerical model.

In the second phase of this study, the heat transfer model was extended to predict the onset of first- and second-degree burns. This was achieved by coupling the multilayer garment heat transfer model with a bioheat transfer model representing human skin. To simulate realistic physiological conditions, the calorimeter and insulation board were replaced with a three-layer skin structure comprising the epidermis, dermis, and subcutaneous tissue. Heat transfer within the skin was modeled using the Pennes bioheat equation.

An air gap of 1 mm was assumed between the inner surface of the garment and the skin, and both conductive and radiative heat transfer mechanisms through the air gap were accounted for, following the methodology outlined in references [81] [82].

Figure 5 illustrates the temperature evolution of the basal layer (interface between epidermis and dermis) as a function of time, for incident heat fluxes ranging from 400 to 1200 W/m². It is observed that the basal layer temperature exceeds the critical threshold of 44 °C—associated with potential skin damage—only when the incident heat flux reaches or exceeds 1000 W/m².

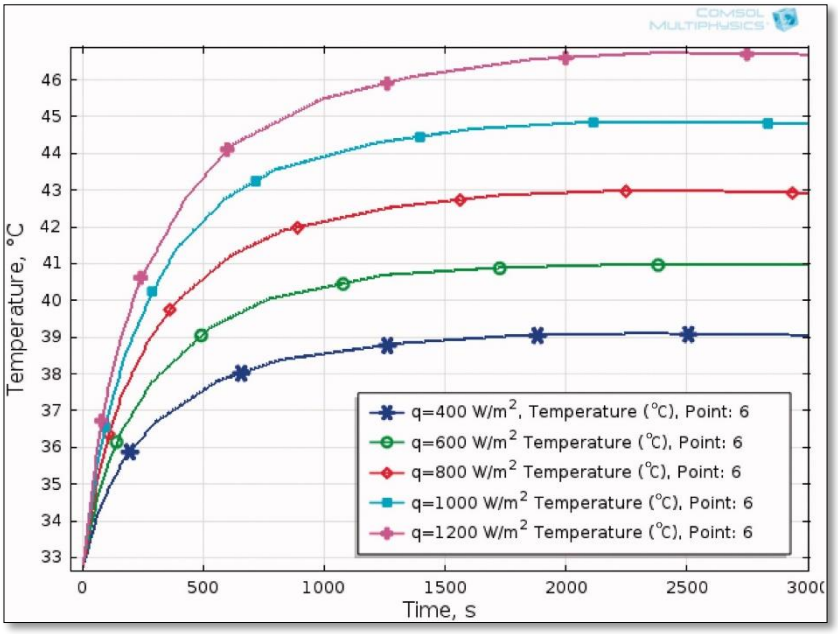

Figure II-7 : Influence of the heat flux on the temperature of the basal layer for a three-layer system and 1-mm air gap between the fabric and the skin. [98]

At an incident radiant heat flux of 1200 W/m², the onset of a first-degree burn is predicted to occur after 32 minutes and 20 seconds of exposure, while the development of a second-degree burn is estimated at 38 minutes and 10 seconds.

The thickness of the air gap between the protective garment and the skin varies depending on anatomical location. According to the findings of Song [83] [84], the largest air gaps are typically observed in the leg region (ranging from 15 to 22 mm), while the smallest occur around the shoulders (approximately 1.6 mm).

Figure 6 illustrates the temperature evolution of the basal skin layer over time under a heat flux of 1200 W/m², for various air gap thicknesses ranging from 1 to 6 mm. The results demonstrate the influence of air gap size on thermal insulation performance and skin temperature response.

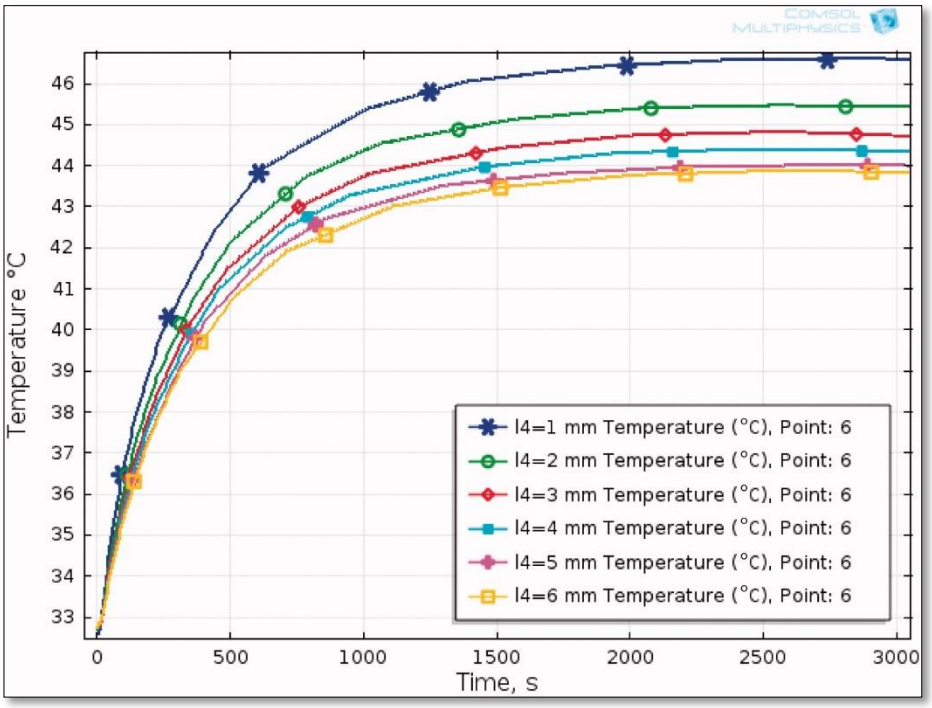

Figure II-8 : Influence of the air gap width on the temperature of the basal layer for a three-layer system and 1200 W/m2 inward heat flux. [101]

An increase of 5 mm in the air gap thickness between the garment and the skin results in a reduction of the basal layer temperature by approximately 2.7 °C. This is attributed to the insulating properties of air, which effectively retard heat transfer; thus, enlarging the air gap enhances thermal insulation and delays heat propagation to the skin.

For an incident heat flux of 1200 W/m², increasing the air gap to 3 mm significantly extends the protection time. The predicted exposure time before the onset of first-degree burns doubled—rising to 65 minutes and 40 seconds—compared to 32 minutes and 20 seconds with a 1 mm air gap. Similarly, the time to second-degree burns increased to 91 minutes and 20 seconds, underscoring the critical role of air gap thickness in thermal protection.

These results confirm that even at relatively low levels of radiant heat exposure, a conventional three-layer thermal protective clothing system is essential to prevent burn injuries. However, it is important to note that the tests were conducted under laboratory conditions at room temperature (approximately 20 °C), which was also the ambient temperature used in the numerical simulations. As such, the outcomes may not fully represent the material behavior under elevated ambient

temperatures and should be interpreted with caution when predicting performance in real-world firefighting scenarios.

The developed numerical model serves as a valuable tool for the design and evaluation of protective clothing systems. It allows for the assessment of how various parameters—including fabric thickness and density, thermal properties (e.g., thermal conductivity, specific heat capacity), optical characteristics, air gap width, and environmental conditions such as radiant heat flux and ambient temperature—influence the protective performance of clothing.

Beyond analyzing material properties, the model can predict the thermal protective performance of fabric systems in terms of skin burn injury. Using a three-layer skin representation, it enables the estimation of the minimum exposure time required to induce second-degree burns, thereby offering critical insights for optimizing protective clothing design and investigating factors that contribute to firefighter burn injuries.

Study Example:

A fire simulation console app modeled the thermal response of firefighter clothing under varying flame intensities (5–20 kW/m²). Results were consistent with burn injury thresholds and supported garment redesign for high-risk environments.

Table II-6 : Summary of Experimental and Numerical Studies.

Study Type	Software	Layers Simulated	Max. Heat Flux Tested	Key Output
1D Heat Transfer	MATLAB	4 (Outer shell, MB, TL, Skin)	8.5 kW/m²	Skin temp over time
Real-time CLI tool	Console (Python/Fortran)	3+	20 kW/m²	Burn threshold zones
Manikin Test	N/A	Full turnout suit	10 kW/m²	Heat flux & T profiles

Both experimental and numerical approaches are essential for improving the design and performance of firefighter protective clothing. MATLAB remains a powerful platform for simulating the thermal behavior of multilayer systems due to its strong numerical libraries and ease of visualizing results.

4. Conclusion :

This chapter reflected on the latest studies on firefighter protective clothing with a focus on the behavior of fires, mechanisms of burn injury, and thermal performance of multi-layered clothing. Studies revealed that thermal protection and comfort were significantly affected by fabric composition, depth of air pocket, and moisture retention.

Experimental findings highlighted that even though protective clothing does not significantly alter physiological strain, fabric properties influence sweat evaporation and comfort perceptions. Amongst the studied ensembles, those with better moisture management (like PPC#1) had better performance.

Computational simulations with the aid of MATLAB and COMSOL were successful in simulating heat transfer and burn risk. The work of Su et al. (2016) was significant in adding compression effects, thus increasing the realism and validity of similar models.

In a nutshell, the integration of numerical and experimental methods is critical for creating protective clothing that addresses safety and physiological efficacy simultaneously in firefighting conditions.

Chapter III
Experimental Tests

III. Chapter 03 : Experimental tests

INTERNSHIP:

I. Presentation of CNTC:

The CNTC Spa Boumerdes is a Support Centre for industry in all branches with the Quality Label (ISO 9001/2008 certification). As such, it is structured to take charge of any management study related to any branch of activity as well as the support of companies in their certification or accreditation process according to ISO 9001,14001...

Moreover, the existence of its ISO 9000 certified laboratories allows it to provide various services specific to industrial branches, as well as any service activity in relation with them, particularly for the Textiles-Plastics-Toys-Water Industry.

The know-how, experience and skills of a pool of high-level experts have enabled the CNTC to perform various services in sectors other than those falling within the field of leather; in particular in the Upgrading, Business Evaluation, Strategic Diagnostics and Recovery Plans activity niches which have mainly targeted the sectors:

- Companies in the chemical and petrochemical sector,
- Cellulose industry,
- Hospitality industry,
- Food industry,
- Buildings and Public Works,
- Cosmetics, etc...

II. History:

The CNTC was created on 30 May 1998 by decision of the Extraordinary General Assembly of the Holding Manufacturing Industry - HOLDMAN, held on 29 April 1998, from the skills and assets of ENEDIM to be transferred in 1999to Holding AGROMAN then to SGP DIPREST in May 2002.

Created in the form of a Joint Stock Company with a capital of 13,000,000 DA increased to 20,000,000DA since 24/08/2004, 100% owned by S.G.P DIPREST.

It will soon be set up as a Support Services Centre for the CTI industry, with the task of providing its services to all branches of activity and particularly the Manufacturing Industry Branch.

The CNTC has a total staff of 72, including 31 university engineers and 14 senior technicians

III. CNTC Missions:

III.1 Engineering and Consulting:

-upgrading of enterprises and institutions.

-Support for certification and accreditation.

-the evaluation of the company in the context of privatisations.

-re-evaluations of business activities.

-environmental studies.

-studies of transport and traffic plans.

-studies of household surveys oriented transport.

-organization studies and implementation of management procedures and audits.

-studies of land use planning schemes

-Architectural studies and project monitoring

III.2 Laboratory activities:

The CNTC has 5 laboratories for control and compliance analysis certified by ISO 9001 and approved by the Ministry of Commerce:

1. textile laboratory for:

- Tests Materials

-Mechanical and Physical Testing

-Physico-chemical tests

- Conformity and Quality Testing

-Fire Behaviour

- Colorimetry

2. leather/plastics/rubber laboratories

3. toy laboratories

4. chemistry laboratories

5. metrology laboratories (ISO 17025 accredited)

IV. Clothing manufacturing:

Clothing manufacturing is the process of turning raw materials into finished garments through a series of well-defined steps such as designing, fabric cutting, sewing, and finishing. At the core of this industry are textile fibers, which serve as the fundamental building blocks of all clothing. These fibers—whether natural (like cotton, wool, and silk) or synthetic (like polyester and nylon)—are spun into yarns and woven or knitted into fabrics that are later transformed into apparel.

IV.1. Textile fibers:

Textile fibers divide to types natural and synthetic.

IV.1.1. Natural:

IV.1.1.1. Plant origin:

Cellulose.

Cotton.

Linen.

Hemp.

Other fibers .

IV.1.1.2. Animal origin:

Wool.

Silk.

Protein fibers.

Other fibers.

IV.1.2. Synthetic:

Polyester.

Polyamide.

Acrylic.

Polyethylene.

Aramid.

Other fibers.

V. Aramid fibers and Firefighter's protective clothing assembly:

Aramid fibres (abbreviation of "aromatic polyamide") are highly heat-resistant synthetic fibres often used in protective clothing (such as firefighter's uniforms, body armor, etc.). There are two main types: para-aramides (e.g., Kevlar) and meta-aramides (e.g., Nomex), each with specific chemical and physical properties.

V.1. Chemical characteristics :

Table III-1 : Chemical Properties of Aramid Fibers.

Property	Detail
Chemical structure	Polymers based on aromatic units linked by amide bonds (-CO-NH-)
General formula	[-CO-Ar-NH-Ar-]n where "Ar" is an aromatic nucleus
Chemical resistance	Good resistance to organic solvents, oils, and fuels
Sensitivity	Degraded by strong acids and concentrated bases
Flammability	Self-extinguishing, does not melt (decomposes without fusion)

V.2. Physical characteristics:

Table III-2 : Physical Properties of Aramid Fibers.

Property	Typical Value
Density	Approximately 1.44 g/cm³ (very lightweight)
Tenacity	Up to 3.6 GPa (very high tensile strength)
Elastic modulus	70–130 GPa (depending on the type of aramid)
Elongation at break	Low (2–4% for Kevlar)
Decomposition temperature	Approximately 500–550°C
Moisture absorption	Medium (3–7%)
Natural color	Golden yellow for Kevlar, cream for Nomex

V.3. Comparative table: Meta-aramid vs Para-aramid :

Table III-3 : Comparison of Meta-Aramid and Para-Aramid Fibers.

Property	Meta-aramid (e.g., Nomex®)	Para-aramid (e.g., Kevlar®)
Structure	Amide bonds in the meta position on the aromatic ring	Amide bonds in the para position
Density	~1.38 g/cm³	~1.44 g/cm³
Tenacity (tensile strength)	Medium (~0.3–0.5 GPa)	Very high (~3.6 GPa)
Elastic modulus	~2.5 GPa	~70–130 GPa
Elongation at break	~20–30%	~2–4%
Thermal resistance	Decomposition around 370–400°C	Decomposition around 500–550°C
Flammability	Self-extinguishing, flame-resistant	Self-extinguishing, highly flame-resistant
Moisture absorption	Medium (4–6%)	Medium (3–7%)
Chemical resistance	Good resistance to solvents, weak against concentrated acids/bases	Same, slightly more sensitive to long-term humidity
Natural color	Cream/off-white	Golden yellow
Typical applications	Heat-protective clothing (firefighters, industry), electrical insulation	Bulletproof vests, cables, reinforced tires, high-performance composites

-Technical explanation:

Para-aramid (Kevlar®) has a rigid linear structure thanks to the perfect alignment of polymer chains resulting in very high mechanical strength.

Meta-aramid (Nomex®) has a more tortuous structure, making it less mechanically resistant but more flexible and very stable at high temperatures.

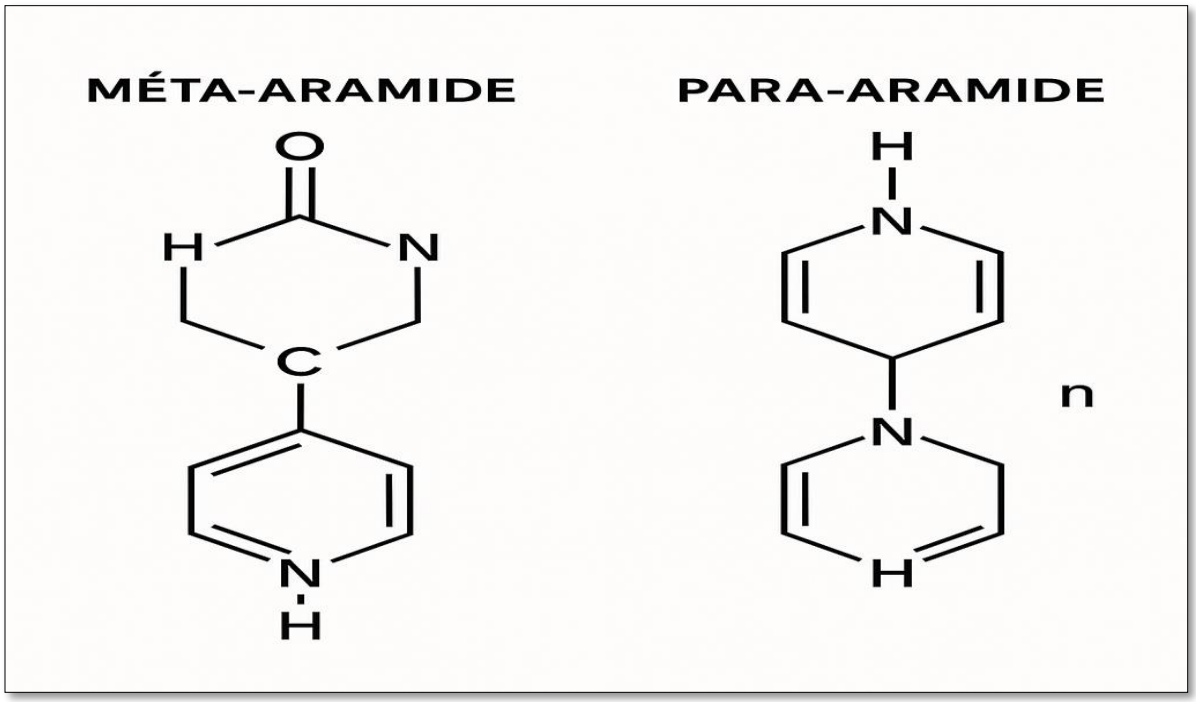

Figure III-1 : Schematic diagram of chemical structures.

VI.Clothing experimental tests:

VI.1. Chemical test :

Objective

To determine the mass percentage of aramid and viscose in a textile sample (warp/weft) by exploiting the selective solubility of viscose in concentrated sulfuric acid.

Materials and Equipment:

● Electronic scale : Electronic Scale 160 (high-precision)

Figure III-2 : Electronic Scale 160 (high-precision)

● Drying oven : NUIVERSEUE OVEN 108 MEMME

Figure III-3 : Drying oven NUIVERSEUE OVEN 108 MEMME

● Desiccator : Standard glass desiccator with silica gel

Figure III-4 : Desiccator Standard glass desiccator with silica gel

● Water bath: 29L stainless steel with temperature control

Figure III-5 : Water bath 29L stainless steel with temperature control

● Beakers : Borosilicate glass

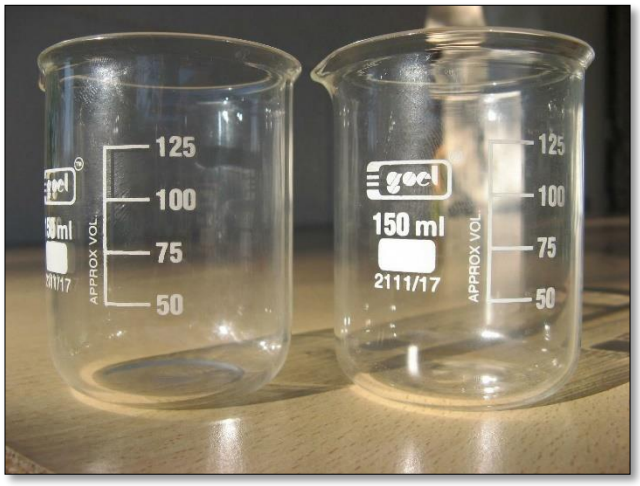

Figure III-6 : Beakers Borosilicate glass

● Sulfuric acid (H_2SO_4) : Concentrated (98%)

● Distilled water : Distilled water

Test Procedure:

Step 1 – Sample Preparation

Cut 1.00 g of textile fibers (separately for warp and weft).

Cut fibers into small pieces.

Weigh the samples using a precision scale (Electronic Scale 160).

Step 2 – Drying

- Place the samples in the NUIVERSEUE OVEN 108 MEMME.
- Temperature: 105°C for 4 hours, to remove moisture without damaging the fibers.

Step 3 – Conditioning

- Immediately transfer the fibers into a desiccator to prevent moisture absorption.
- Leave the fibers in the desiccator for 30 to 60 minutes to reach equilibrium.
- Mass after conditioning: 0.95 g.

Step 4 – Preparation of 75% Sulfuric Acid Solution

- Pour 350 mL of distilled water into a large beaker.
- Slowly add 700 mL of concentrated sulfuric acid (98%) to the water (acid into water, never the reverse) to avoid violent reactions.

Safety note: Perform this step under a fume hood with full PPE (gloves, goggles, lab coat).

Step 5 – Chemical Treatment of Fibers

- Place the dried fibers in separate beakers.
- Add the 75% sulfuric acid solution until fibers are fully submerged.
- Place the beakers in a temperature-controlled water bath at 50°C ± 5°C.
- Duration: 1 hour, with gentle manual stirring every 10 minutes.

Scientific note: Viscose (regenerated cellulose) is soluble in 75% sulfuric acid, while aramid fibers (e.g., Kevlar, Nomex) are resistant.

Final Analysis

After treatment:

1. Filter the insoluble residue (aramid).
2. Rinse thoroughly with distilled water.
3. Dry the residue in the oven again.
4. Condition in the desiccator and weigh.

Composition Calculation

- **% Aramid** = (Dry residue mass after treatment / Initial dry mass) × 100
- **% Viscose** = 100 − % Aramid

VI.2.Cloth test with flame :

Objective : To evaluate the flame resistance and limited flame spread properties of a textile composed of 50% aramid and 50% viscose using a controlled laboratory flame exposure test.

Materials and Equipment:

● Test samples of fabric (50% aramid, 50% viscose), dimensions: (200mm x 150 mm).

● Flame application device (Flammability tester).

Figure III-7 : Flammability tester.

●Frame for mounting specimens (vertical orientation).

Figure III-8 : Frame for mounting specimens.

● Stopwatch.

Figure III-9 : Stopwatch.

●Ruler or calipers.

● Conditioning chamber (20 ± 2°C and 65 ± 5% relative humidity).

● Heat-resistant gloves and safety equipment.

●Ignition source: butane flame (60mm length).

Test Procedure:

Ignition Methods:

A. Edge Ignition (Procedure A)

● Apply a 60 mm butane flame to the bottom edge of the vertically suspended specimen for 20 seconds.

B. Surface Ignition (Procedure B)

● Apply the flame perpendicularly to the surface (center of the fabric) for 20 seconds.

Observe and Record:

Charring and dark brown/black discoloration.

More charring on the exposed side, with visible carbon residue.

Differential shrinkage due to the blend can cause fabric puckering or wrinkling.

Fabric shrink or deform unevenly, especially in flame contact area.

Viscose combustion releases acrid, cellulose-burning smell and visible smoke.

Aramid gives less smoke and different odor when degrading.

Criteria for Evaluation:

According to ISO 15025:2016, the fabric passes if:

Afterflame time: ≤ 2 seconds

Afterglow time: ≤ 2 seconds

No hole formation that reaches edge of specimen

No flaming or molten debris

Charring length: within specified limits (<150 mm)

Expectations:

- If exposure time or heat flux is sufficient (more than 20 seconds), viscose regions may ignite or break down fully, forming holes.
- Viscose is thermoplastic and loses strength rapidly under heat, while aramid maintains integrity.
- Aramid may resist ignition but can still degrade.

Results :

- Real-world damage depends on flame exposure time, heat flux, fabric weight (gsm), and air gap between fabric and flame.
- Blends like 50/50 are compromises between comfort and protection, and which meet with firefighting standards.

Results from all the Internship:

Firefighters' clothing consists of three layers:

1- Outer layer (100% aramid)

2- Moisture barrier

3- Thermal barrier

The firefighters' clothing must not be heavy, breathable, heat-stable and chemically anti-humidity clothing.

Textile mix plays an important role in the comfort and protection of the firefighter.

Blended fabrics can be used in inner layers, not in direct contact with flame.

The textile mix is critical – blends can enhance comfort but must be carefully positioned within the layering system to avoid compromising safety.

Clothing must be lightweight enough to prevent fatigue but dense enough to resist heat.

Performance: Aramid fibers char rather than melt or drip, providing exceptional flame resistance above 400°C.

VII. Conclusion :

This chapter detailed the experimental evaluation of firefighter protective clothing, focusing on the material properties and flame resistance of aramid-based fabrics. Through chemical testing, the composition of fabric blends was accurately determined using selective dissolution techniques. Flame spread tests, conducted under ISO 15025:2016 standards, confirmed the superior flame resistance of aramid fibers compared to viscose, which showed faster degradation and smoke production.

The results demonstrated that blends such as 50% aramid / 50% viscose offer a compromise between comfort and protection but must be carefully integrated within the garment’s layering system. Aramid fibers, due to their high thermal stability and non-melting behavior, are best suited for outer layers exposed directly to heat. Proper design of the clothing system—including moisture and thermal barriers—is essential to ensure breathability, mechanical integrity, and thermal protection.

Overall, the experiments validated the importance of fiber selection and fabric architecture in optimizing both the protective and physiological performance of firefighter gear.

Chapter IV

Formulation and thermal balance equations.

IV. Chapter 04: Formulation and thermal balance equations.

1. Introduction

In this chapter, we describe the mathematical formulation used for the analysis of the thermal response of the firefighter protective body-clothing system. The model is established in order to model the heat transfer through the multilayered clothing and its interaction with the skin under fire exposure conditions. The formulation accounts for the three major modes of heat transfer—conduction, convection, and radiation—and uses proven principles of biothermics and thermodynamics.

2. Heat balance equations

2.1. Cases schemas

In this study, we model the heat transfer through a three-layer firefighter protective jacket and the resulting thermal skin injuries under a one-dimensional thermal exposure scenario. Numerical simulations are performed using MATLAB.

The core of this chapter focuses on two mathematical models that describe the temperature distribution across both the protective clothing layers and the skin tissues. The skin is modeled as comprising five homogeneous regions — the epidermis, dermis, subcutaneous tissue, muscle, and bone — each characterized by its specific thermal and physiological properties. The heat source is assumed to be located in front of the outermost layer of the protective jacket.

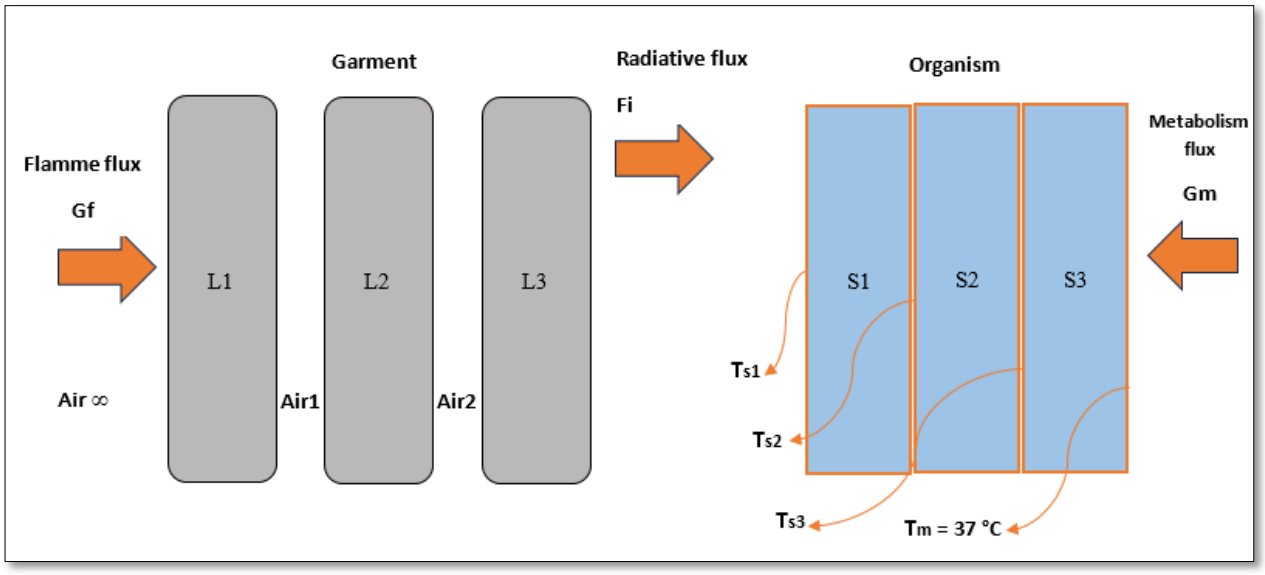

Figure IV-1 : The holding layers and the skin and their different heat exchange.

2.2. Heat transfer phenomena

Heat transfer is a fundamental concept in fire safety engineering, as it governs the transmission of thermal energy between different regions. This phenomenon significantly influences fire propagation within buildings and directly impacts the effectiveness of implemented safety measures. A comprehensive understanding of heat transfer mechanisms is essential for engineers to design fire-resilient structures and to develop more efficient fire protection strategies.

In the context of fire safety, heat transfer occurs through three principal modes: conduction, convection, and radiation. Each mechanism contributes differently to the behavior and progression of fire within an environment.

Conduction: Refers to the transfer of heat through solid materials. In building structures, this mode of heat transfer can occur through components such as walls, floors, and ceilings, thereby facilitating the spread of fire to adjacent areas within the structure.

Convection: Convection is the process of heat transfer through fluids, including both liquids and gases. In fire scenarios, this mechanism is particularly significant, as the upward movement of hot gases and the downward flow of cooler gases contribute to the dynamic behavior of fire.

Convective heat transfer plays a critical role in fire propagation by transporting hot smoke, gases, and flames to previously unaffected areas.

Radiation: Radiation refers to the emission and transmission of thermal energy in the form of electromagnetic waves. In the context of fire, radiative heat is dispersed in all directions and has the potential to ignite nearby combustible materials without the need for direct contact, thereby contributing to the rapid spread of fire. [85]

2.3. Heat transfer phenomena equations

2.3.1. Modeling Heat Balances and Algebraic Equations:

2.3.1.1. Heat Balances for the Unsteady Case:

In the unsteady state, the heat balance is written as follows:

$$\Phi_{received} - \Phi_{lost} = \frac{d}{dt}(accumulated\ heat) \qquad (IV.1)$$

Now the heat accumulated per unit of surface is written as follows:

$$\frac{d}{dt}(accumulated\ heat) = \frac{d}{dt}(\rho * cp * T) * \Delta x \qquad (IV.2)$$

So the unsteady balance is:

$$\sum \Phi_{received} - \sum \Phi_{lost} = (\rho_{Li} * cp_{Li} * epv_{Li}) * \frac{dT_{Li}}{dt} \qquad (IV.3)$$

ρ_{Li}: Density of tissues in the layer Li/skin

cp_{Li}: Specific heat of the tissues of the layer Li/skin

epv_{Li}: Thickness of the layer Li/skin

T_{Li}: Layer temperature Li/skin

Balance of layer 1

A. Flows received:

$$\Phi_{f\rightarrow L1} = \alpha_{L1} * G_f \quad \text{(IV. 4)}$$

B. Lost flows:

B.1 Radiation L1↔L2

$$\Phi_{L1\rightarrow L2}^{Rad} = \sigma * \varepsilon_{L1L2}(T_{L1}^4 - T_{L2}^4) \quad \text{(IV. 5)}$$

B.2 Convection L1→L2

$$\Phi_{L1\rightarrow L2}^{Conv} = h_{L1L2}(T_{L1} - T_{L2}) \quad \text{(IV. 6)}$$

B.3 Radiation: Reflection Gf

$$\Phi_{L1\rightarrow flame} = R_{L1} * G_f \quad \text{(IV. 7)}$$

B.4 Convection L1→∞

$$\Phi_{L1\to\infty}^{Conv} = I_{Conv\infty} * h_{L1\infty}(T_{L1} - T_{\infty}) \quad (IV.8)$$

B.5 Radiation: L1→∞

$$\Phi_{L1\to\infty}^{Rad} = I_{rad\infty} * \sigma * \varepsilon_{L1}(T_{L1}^4 - T_{\infty}^4) \quad (IV.9)$$

B.6 Conduction: L1⇔L2

$$\begin{cases} \Phi_{L1\to L2}^{Cond} = I_{Cond1} * \dfrac{T_{L1} - T_{L2}}{R_1} \\ R_1 = \dfrac{ep_1}{\lambda_{air1}} \end{cases} \quad (IV.10)$$

By applying balance I to layer L1 we will have:

$$\alpha_{L1} * G_f - I_{Conv\infty} * h_{L1\infty}(T_{L1} - T_{\infty}) - I_{rad\infty} * \sigma * \varepsilon_{L1}(T_{L1}^4 - T_{\infty}^4) - I_{Cond1} * \frac{T_{L1} - T_{L2}}{R_1} - \sigma * \varepsilon_{L1L2}(T_{L1}^4 - T_{L2}^4) - h_{L1L2}(T_{L1} - T_{L2}) - R_{L1} * G_f = (\rho_{L1} * cp_{L1} * epv_{L1}) * \frac{dT_{L1}}{dt} \quad (IV.11)$$

In compact writing we will have:

$$\frac{dT_{L1}}{dt} = \left[\frac{1}{\rho_{L1} * cp_{L1} * epv_{L1}}\right] * \{(\alpha_{L1} - R_{L1}) * G_f - I_{Conv\infty} * h_{L1\infty}(T_{L1} - T_{\infty}) - I_{rad\infty} * \sigma * \varepsilon_{L1}(T_{L1}^4 - T_{\infty}^4) - \sigma * \varepsilon_{L1L2}(T_{L1}^4 - T_{L2}^4) - \left(\frac{I_{Cond1}}{R_1} + h_{L1}\right) * (T_{L1} - T_{L2})\} \quad (IV.12)$$

Balance of layer 2 L2 :

A. Flows received:

A.1 Flame→

$$\Phi_{f\to L2} = \alpha_{L2} * \tau_{L1} * G_f \quad \text{(IV. 13)}$$

A.2 Convection L1→L2

$$\Phi_{L1\to L2}^{Conv} = h_{L2L1} * (T_{L1} - T_{L2}) \quad \text{(IV. 14)}$$

A.3 Radiation L1→L2

$$\Phi_{L1\to L2}^{Rad} = \sigma * \varepsilon_{L2L1} * (T_{L1}^4 - T_{L2}^4) \quad \text{(IV. 15)}$$

B. Lost flows:

B.1 Radiation L2→L3

$$\Phi_{L2\to L3}^{Rad} = \sigma * \varepsilon_{L2L3} * (T_{L2}^4 - T_{L3}^4) \quad \text{(IV. 16)}$$

B.2 Convection L2→L3

$$\Phi_{L2\to L3}^{Conv} = h_{L2L3} * (T_{L2} - T_{L3}) \quad \text{(IV. 17)}$$

B.3 Air2 conduction L2→L3

$$\begin{cases} \Phi_{L2\to L3}^{Cond} = \dfrac{T_{L2} - T_{L3}}{R_2} * I_{Cond2} \\ R_2 = \dfrac{ep_2}{\lambda_{air2}} \end{cases} \quad \text{(IV. 18)}$$

Applying balance I to layer L 2

$$\frac{dT_{L2}}{dt} = \left[\frac{1}{\rho_{L2} * cp_{L2} * epv_{L2}}\right] * \{(\alpha_{L2} * \tau_{L1} * G_f) + h_{L2L1} * (T_{L1} - T_{L2}) + \sigma * \varepsilon_{L2L1} * (T_{L1}^4 - T_{L2}^4) + \sigma * \varepsilon_{L2L3} * (T_{L3}^4 - T_{L2}^4) + \left(h_{L2L3} + \frac{I_{Cond2}}{R_2}\right) * (T_{L3} - T_{L2})\} \quad (IV.19)$$

Balance of layer 3 L3

A. Flows received:

A.1 Flame→L3

$$\Phi_{f\to L3} = \alpha_{L3} * (\tau_{L2} * \tau_{L1}) * G_f \quad (IV.20)$$

A.2 Skin →L3

$$\Phi_{P\to L3} = \alpha_{L3} * G_i \quad (IV.21)$$

A.3 Convection L2→L3

$$\Phi_{L2\to L3}^{Conv} = h_{L3L2} * (T_{L2} - T_{L3}) \quad (IV.22)$$

A.4 L2→L3 radiation

$$\Phi_{L2\to L3}^{Rad} = \sigma * \varepsilon_{L2L3} * (T_{L2}^4 - T_{L3}^4) \quad (IV.23)$$

B. Lost flows:

B.1 Air 3 conduction L3→Skin

$$\begin{cases} \Phi_{L2\to L3}^{Cond} = I_{Cond3} * \dfrac{T_3 - T_p}{R_3} \\ R_3 = \dfrac{ep_3}{\lambda_{air3}} \end{cases} \quad (IV.24)$$

B.2 Convection L3→Skin

$$\Phi_{L3\to P}^{Conv} = h_{L3P} * (T_3 - T_P) \quad (IV.25)$$

B.3 Radiation L3→Skin

$$\Phi_{L3\to P}^{Rad} = \sigma * \varepsilon_{L3P} * (T_{L3}^4 - T_P^4) \quad (IV.26)$$

Balance sheet I applied to L3 gives:

$$\frac{dT_{L3}}{dt} = \left[\frac{1}{\rho_{L3} * cp_{L3} * epv_{L3}}\right] * \{(\alpha_{L3} * \tau_{L2} * \tau_{L1}) * G_f + \alpha_{L3} * G_i + h_{L3L2} * (T_{L2} - T_{L3}) + \sigma * \varepsilon_{L2L3} * (T_{L2}^4 - T_{L3}^4) - \sigma * \varepsilon_{L3P} * (T_{L3}^4 - T_P^4) - \left(h_{L3P} + \frac{I_{Cond3}}{R_3}\right) * (T_{L3} - T_P)\} \quad (IV.27)$$

2.3.1.2. Skin layer balance :

Balance on the S1 skin layer

A. Flows received:

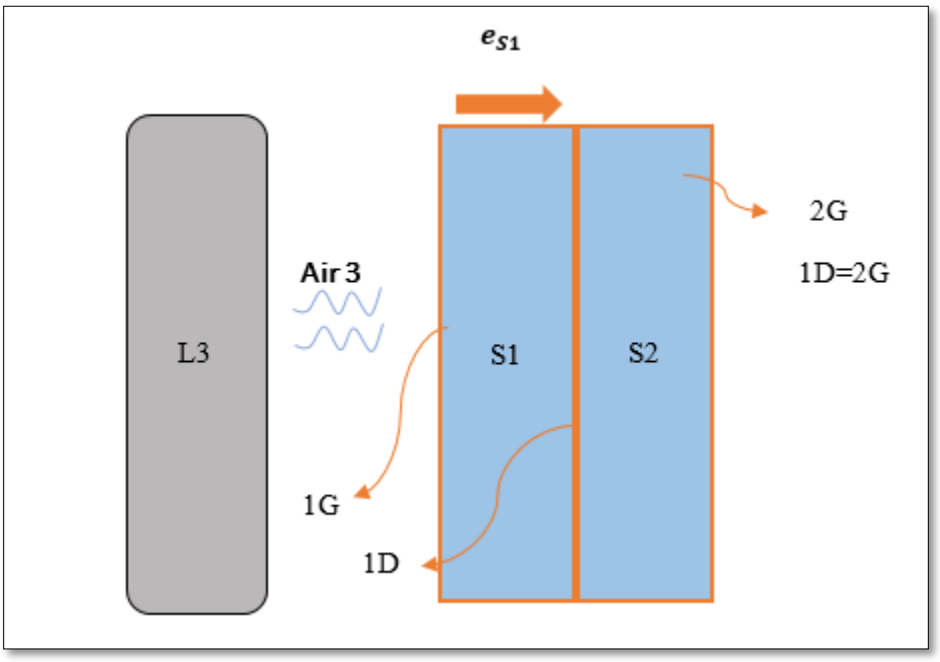

Figure IV-2 : 1D diagram of heat transfers [balances on layer S1]

A.1 Convection flow: L3→ S1

$$\Phi_{L3\rightarrow S1}^{conv} = h_{S1} * (T_{L3-}T_{S1G}) \qquad (IV.28)$$

A.2 Radiation Flux L3 →S1

$$\Phi_{L3\rightarrow S1}^{rad} = \sigma * \varepsilon_{L3L1} * (T_{L3}^4 - T_{S1G}^4) \qquad (IV.29)$$

A.3 flame→S1

$$\Phi_{flame\rightarrow S1} = \alpha_{S1*}(\tau_{L3} * \tau_{L2}\tau *_{L1}) * G_f \quad (IV.30)$$

A.4 F metabolism m →S1

$$\Phi_{m\rightarrow S1} = \alpha_{S1} * (\tau_{S3} * \tau_{S2}) * G_m \quad (IV.31)$$

B. Lost flows:

B.1 Evaporation flow S1 →Air 3

$\Phi_{S1\ Air3}=G_{evp}$

B.2 Flux conduction S1 →S2

$$\begin{cases} \Phi_{S1Air3} = \dfrac{T_{S1G}-T_{S2G}}{\dfrac{e_{S1}}{\lambda_{S1}}} \\ R_{S1} = \dfrac{e_{S1}}{\lambda_{S1}} \end{cases} \quad (IV.32)$$

By applying the unsteady to the S1 layer

$$\frac{dT_{S1G}}{dT} = \left(\frac{1}{\rho_{L2*}cp_{L2*}e_{L2}}\right) * \left\{h_{S1} * (T_{L3}-T_{S1G}) + \sigma * \varepsilon_{L3S1} * (T_{L3}^4-T_{S1G}^4) + \alpha_{S1\rightarrow}(\tau_{L3*}\tau_{L2} * \tau_{L1}) * G_f + \alpha_{S1} * (\tau_{S3} * \tau_{S2}) * G_m - G_{evp} - \frac{1}{R_{S1}} * (T_{S1G} - T_{S2G})\right\} \quad (IV.33)$$

Balance sheet on the S2 layer

A. Flows received:

A.1 Flame →S2

E) balance sheet on the S2 layer

A. Flows received:

A.1 Flame →S2

$$\Phi_{f\to S2} = \alpha_{S2} * (\tau_{S1} * \tau_{L3} * \tau_{L2*}\tau_{L1}) \quad (IV.34)$$

A.2 metabolism →S2

$$\Phi_{mS\to 2} = \alpha_{S2} * (\tau_{S3}) * G_m \quad (IV.35)$$

A.3 Conduction flow S1→S2

$$\Phi_{S1\to S2} = \frac{1}{R_{S1}} * (T_{S1G} - T_{S2G}) \quad (IV.36)$$

B. Lost flows:

B.1 Conduction flow S2 →S3

$$\begin{cases} \Phi_{S2\to S3} = \dfrac{1}{R_{S2}} * (T_{S2G} - T_{S3G}) \\ R_{S2} = \dfrac{e_{S2}}{\lambda_{S2}} \end{cases} \quad (IV.37)$$

Applying the unsteady balance on the S2 layer is written

$$\frac{dT_{S2G}}{dt} = \left[\frac{1}{\rho_{S2} cp_{S2} e_{S2}}\right] * \left\{(\alpha_{S2} * (\tau_{S1} * \tau_{L3} * \tau_{L3}\tau_{C4}) * G_f) + \alpha_{S2} * \tau_{S3} * G_m + \frac{1}{R_{S1}} * (T_{S1G} - T_{S2G}) - \frac{1}{R_{S2}} * (T_{S2G} - T_{S3G})\right\} \quad (IV.38)$$

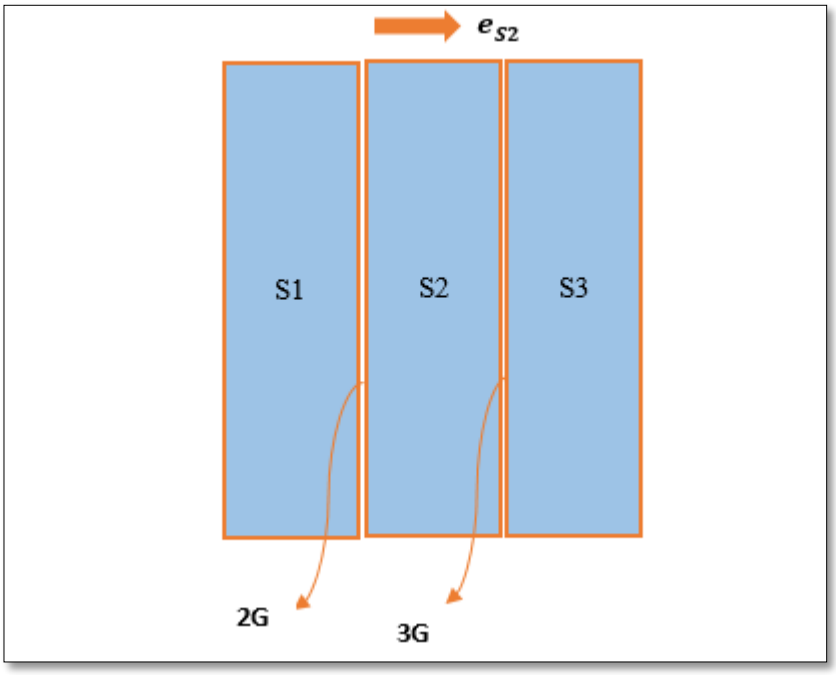

Figure IV-3: 1D diagram of heat transfer (balances on the S2 layer)

Balance sheet on the S3 layer

A. Flows received:

A.1 Flame →S3

$$\Phi_{f \to S3} = \alpha_{S3} * (\tau_{S2} * \tau_{S1} * \tau_{L3}\tau_{L2} * \tau_{L1}) * G_f \quad (IV.39)$$

A.2 metabolism →S3

$$\Phi_{f\rightarrow S3} = \alpha_{S3} * G_m \qquad (IV.40)$$

A.3 Conduction flow S2→S3

$$\Phi_{S2S3} = \frac{1}{R_{S2}}(T_{S2G} - T_{S3G}) \qquad (IV.41)$$

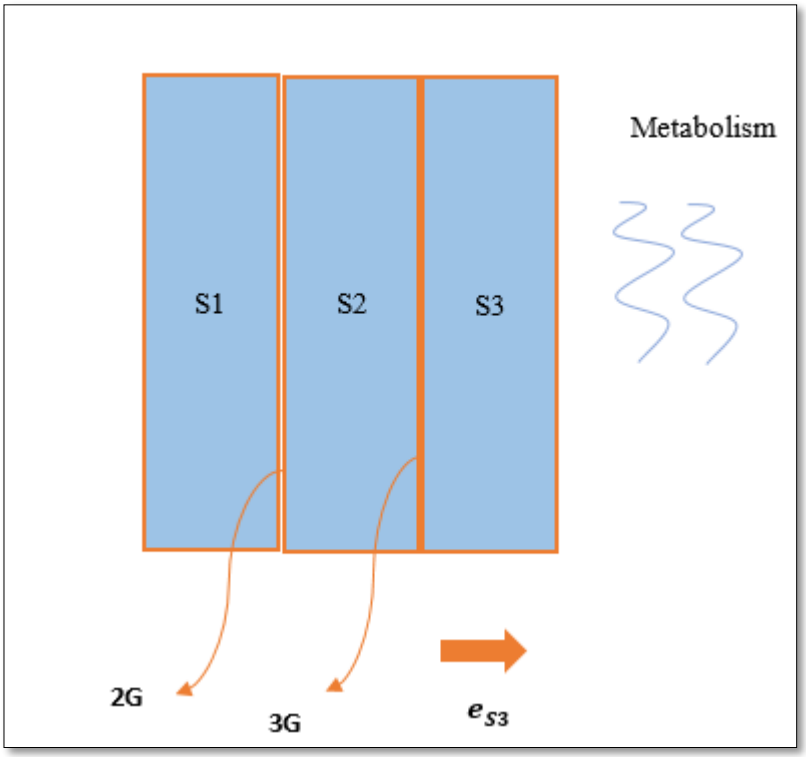

Figure IV-4 : 1D diagram of heat transfers [balances on layer S3]

B. Lost flows:

B.1 conduction flow towards the organism (metabolism)

$$\begin{cases} \Phi_{S3\to m} = \dfrac{1}{R_{S3}}(T_{S3G} - T_m) \\ R_{S3} = \dfrac{e_{S3}}{\lambda_{S3}} \end{cases} \quad \text{(IV. 42)}$$

Applying the unsteady balance on the S3 layer is written

$$\frac{dT_{S3G}}{dt} = \left[\frac{1}{\rho_{S3} * cp_{S3} * e_{S3}}\right] * \left\{\alpha_{S3}(\tau_{S2} * \tau_{S1} * \tau_{L3} * \tau_{L2} * \tau_{L1}) * G_f + \alpha_{S3} G_m + \frac{1}{R_{S2}} * (T_{S2G} - T_{S3G}) - \frac{1}{R_{S3}} * (T_{S3H} - T_m)\right\} \quad \text{(IV. 43)}$$

2.3.1.3. Pennes' Bioheat Equation

The first bioheat equation was developed by Pennes in 1948 [86] and remains one of the foundational models in the field of thermal analysis in biological tissues. Although it has been the subject of ongoing debate and criticism over the years, it continues to be widely adopted in mathematical modeling of bioheat transfer.

Heat transfer in living organisms is primarily governed by two mechanisms:

- Blood perfusion**,**
- Metabolic heat generation**.**

Before applying any model, it is crucial to determine the appropriate spatial scale for analyzing temperature distribution, given the complex and hierarchical structure of the vascular network. Pennes' model is most effective at spatial scales ranging from a few millimeters to several centimeters, making it particularly suitable for macroscopic thermal studies in biological tissues. [87]

2.3.1.4. Hypotheses

Pennes proposed that, within a given control volume, the heat transfer q_p between blood and tissue is proportional to the temperature difference between the arterial blood entering the tissue and the venous blood exiting it. This relationship is expressed as:

$$q_p = w(\rho C)_{bl}(T_{art} - T_v) \quad \text{(IV. 44)}$$

Here, the subscript *bl* refers to the thermal properties of blood, and *w* represents the blood perfusion rate [17].

To link the venous blood temperature T_v to the arterial blood temperature T_{art} and the tissue temperature T_t, Pennes introduced a coefficient k', yielding the expression:

$$T_v = T_t + k'(T_{art} - T_v) \tag{IV.45}$$

Two limiting cases help interpret this coefficient:

When $k' = 0$, complete thermal equilibrium is assumed, and the venous blood exits the tissue at the tissue temperature T_t.

When $k' = 1$, there is no thermal exchange between blood and tissue, and the venous blood retains the arterial temperature.

In addition to perfusion, metabolic heat generation is also included in the bioheat equation as a volumetric heat source term:

$$Q_{metb} = Q_0 + Q \tag{IV.46}$$

where

$$Q = Q_0 \cdot 10^{\frac{T_0 - T}{10}} \tag{IV.47}$$

In this expression:

Q_0 represents the basal metabolic heat generation rate at a reference temperature of 36.8°C (or 309.95 K), expressed in W/m³,

T_0 is the reference temperature,

The coefficient $10^{(T_0-T)/10}$ describes the temperature dependence of metabolic heat production, typically ranging between 1 and 2.

Perfusion becomes particularly significant in cases of prolonged thermal exposure where heat fluxes are relatively low. As such, it must be incorporated into skin modeling [16–17]. Blood perfusion is a critical and unique mechanism in bioheat transfer, with blood acting as a volumetric and uniformly distributed heat source in biological tissues [19].

More broadly, the objective is to assess how effectively blood contributes to transporting metabolic heat from the body's interior to the external environment via the skin. This is modeled using Pennes' equation. Upon solving it, it has been demonstrated that blood plays an active role in removing heat from tissues.

Yong-Gang and Liu [20] combined experimental measurements with numerical modeling based on Pennes' equation to show that blood perfusion can be inferred from observed temperature increases. They concluded that higher heat fluxes correlate with increased perfusion, as the body attempts to regulate internal temperature by enhancing blood flow.

3. Computational software (MATLAB)

3.1. Presentation of the computational software (MATLAB)

In order to model and simulate the thermal behavior of a firefighter's protective clothing system, a computational approach is required due to the complexity of the coupled heat transfer mechanisms—conduction, convection, and radiation—across multiple layers with different thermophysical properties. MATLAB (Matrix Laboratory) is chosen as the primary computational software for this study due to its robust numerical computation capabilities, built-in solvers for differential equations, and advanced data visualization tools.

MATLAB is widely used in scientific and engineering disciplines for solving mathematical problems, especially those involving matrix operations, numerical analysis, and differential equations. Its versatility, ease of scripting, and large user base make it a suitable environment for implementing complex heat transfer models.

3.1.1. Objectives of MATLAB Implementation

The implementation of the mathematical model in MATLAB serves several key objectives:

To numerically solve the one-dimensional heat conduction equations in a multilayer system.

To incorporate the effects of surface radiation and external convection into the thermal model.

To simulate transient temperature evolution in each clothing and skin layer during fire exposure.

To detect critical thermal thresholds associated with skin burns.

To allow for parameter variation and case comparison (e.g., fabric thickness, exposure time, etc.).

3.1.2. MATLAB Program Structure

The MATLAB code is organized into modular scripts and functions:

Table IV-1: MATLAB Program Structure.

Section	Description
`init_properties.m`	Defines thermophysical properties of each layer
`boundary_conditions.m`	Applies environmental conditions and initial state
`heat_solver.m`	Executes the RK4 algorithm to compute temperature evolution
`burn_thresholds.m`	Checks when the skin layer exceeds pain and damage temperature thresholds
`plot_results.m`	Generates plots for temperature profiles, thermal flux, and critical times

3.2. Runge-kutta method

The Runge-Kutta methods are a family of iterative techniques used to solve ordinary differential equations (ODEs). Among these, the fourth-order Runge-Kutta method (RK4) is widely used due to its balance between computational efficiency and numerical accuracy. In this study, the RK4 method is employed to integrate the time-dependent heat transfer equations for the multi-layer firefighter protective clothing system. [88]

Theoretical Background

Consider a general first-order ODE:

$$\frac{dy}{dt} = f(t, y), \quad y(t_0) = y_0 \tag{IV.48}$$

The RK4 method approximates the solution at each time step $t_{n+1} = t_n + h$ using the following set of equations:

$$\begin{aligned} k_1 &= f(t_n, y_n) \\ k_2 &= f\left(t_n + \frac{h}{2}, y_n + \frac{h}{2}k_1\right) \\ k_3 &= f\left(t_n + \frac{h}{2}, y_n + \frac{h}{2}k_2\right) \\ k_4 &= f(t_n + h, y_n + hk_3) \\ y_{n+1} &= y_n + \frac{h}{6}(k_1 + 2k_2 + 2k_3 + k_4) \end{aligned} \tag{IV.49}$$

Here, h is the time step, and k_1, k_2, k_3, k_4 are intermediate slopes used to compute a weighted average slope for the step.

Application to Heat Transfer

In the context of transient heat conduction in clothing layers, the temperature at each spatial node i is governed by:

$$\frac{dT_i}{dt} = \frac{k}{\rho c_p}\left(\frac{T_{i+1} - 2T_i + T_{i-1}}{\Delta x^2}\right) + Q_i \qquad (\text{IV.}50)$$

Where:

T_i is the temperature at node i,

Q_i includes contributions from convective and radiative heat transfer,

k, ρ, c_p are material properties.

Each spatial node is treated as a variable in the ODE system. RK4 is applied to update all nodes simultaneously over discrete time steps. This results in a stable and accurate simulation of how heat penetrates through the multilayer system into the skin.

Implementation in MATLAB

In the MATLAB code:

A loop iterates over time using RK4.

At each step, temporary values k_1 through k_4 are calculated for all temperature nodes.

The updated temperatures are stored and used for the next iteration.

The method ensures accurate tracking of rapid temperature changes, which is essential for fire exposure scenarios.

Advantages

Accuracy: Fourth-order convergence allows high precision even with moderate time step sizes.

Stability: Suitable for non-stiff and mildly stiff problems, typical of transient heat conduction.

Ease of implementation: Especially in MATLAB, RK4 is simple to code and debug.

3.3. Matlab program

This study aims to analyze the transient thermal behavior of a multilayer firefighter protective clothing assembly using numerical simulations. The assembly includes multiple textile layers and the skin, and it is subject to a heat flux that may result from fire or elevated ambient conditions. The simulation framework is implemented in MATLAB, comprising three core components:

A main program to define initial conditions and post-process the results.

A numerical solver based on the Fourth-Order Runge-Kutta Method for time integration.

A system of ordinary differential equations (ODEs) that represent energy conservation within each layer.

Each MATLAB script plays a crucial role in the holistic simulation approach, enabling the prediction of temperature evolution across time and depth.

rkgen_PFE.m | unsteady_program_PFE.m | Diff_system1_PFE.m

```
clc; clear all ;close all;

%Provide the Initial Conditions
%T0=[TLay1;TLay2;TLay3;Tskin];
T0=[293;293;293;293;293;293]; %[K]

%Call on Runge-Kutta Function to Perform Integration
 [t,T]=rkgen_PFE('Diff_system1_PFE',[0 1800],T0,0.01);  %15min=900sec, step=0.01

disp('*****Temperatures are in degree Kelvin *****');

fprintf('Time = %5.0f sec\n',t(180001));
fprintf('T_L_1 = %5.4f Â°C\n',T(1,180001)-273);
fprintf('T_L_2 = %5.4f Â°C\n',T(2,180001)-273);
fprintf('T_L_3 = %5.4f Â°C\n',T(3,180001)-273);
fprintf('T_S_1 = %5.4f Â°C\n',T(4,180001)-273);
fprintf('T_S_2 = %5.4f Â°C\n',T(5,180001)-273);
fprintf('T_S_3 = %5.4f Â°C\n',T(6,180001)-273);


figure;
i=1:180001;
plot(t(i),T(1,i)-273,'b-',t(i),T(2,i)-273,'y-',t(i),T(3,i)-273,'r-','LineWidth',1.5);
legend({'T_L_1','T_L_2','T_L_3'},'Location','NorthEast','FontSize',14,'FontWeight','normal','FontAngle','italic');
```

Figure IV-5 : Matlab program.

3.4. Boundary conditions [89] [90] [91]

Table IV-2 : Boundary conditions.

	C1	C2	C3	S1	S2	S3
δ (mm)	0,42	0,75	1,55	0.08	2	10
λ (W/m.°C)	0,081	0,041	0,038	0.225	0.989	0.167
ρ (Kg.m^{-3})	605,0	212,0	112,0	1200	1200	1000
Cp (J/Kg.K)	1187,50	1297,0	1219,0	3598	3222	2760
α /ε	0,98 ; 0,60	0,5 ; 0,60	0,5 ; 0,60	0.97 ; 0.98	0.97	1

Thicknesses of the different air gaps (between layers)

Ep =[0.002; 0.002; 0.005];

Gf=2300; Gm=380.5; Gevap=15.27; [W]

Tamb=298 ; Tm=309.85; [K]

4. Conclusion

In this chapter, a comprehensive mathematical formulation of the thermal response of firefighter protective body-clothing systems was presented. The model integrates the principal heat transfer mechanisms—conduction, convection, and radiation—through a multilayer assembly composed of both textile materials and skin tissues. Detailed heat balance equations for each clothing and skin layer were developed under transient conditions, taking into account complex interactions between external heat fluxes and internal physiological processes such as blood perfusion and metabolic heat generation, modeled through Pennes' bioheat equation.

Furthermore, the computational implementation in MATLAB was elaborated, highlighting the structure of the code, the use of the fourth-order Runge-Kutta method for time integration, and the incorporation of realistic boundary conditions. This numerical approach enables precise tracking of temperature evolution across the multilayer system and the prediction of potential burn injuries under fire exposure. The formulation and simulation tools developed in this chapter provide a solid

foundation for the advanced thermal analysis and optimization of protective clothing, which will be explored further in the subsequent chapter.

Chapter V
Results & discussion

V. Chapter 05: Results and discussion

1. Introduction

This chapter presents the results of the numerical simulation conducted using MATLAB to analyze the thermal behavior of a firefighter protective clothing assembly. The objective is to evaluate the time-dependent temperature profiles across the clothing and skin layers under various exposure conditions. Three case studies are analyzed: a baseline case and two parametric variations. The results are compared to assess the effectiveness of thermal protection and to identify critical parameters influencing thermal insulation and skin safety.

2. Baseline case results

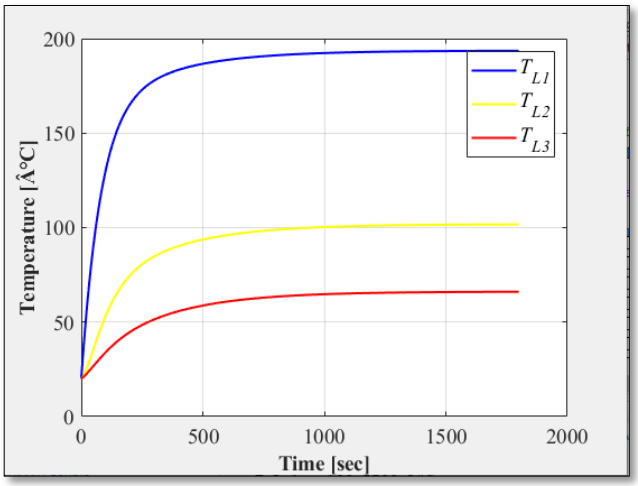

Figure V-1: Baseline results (layers).

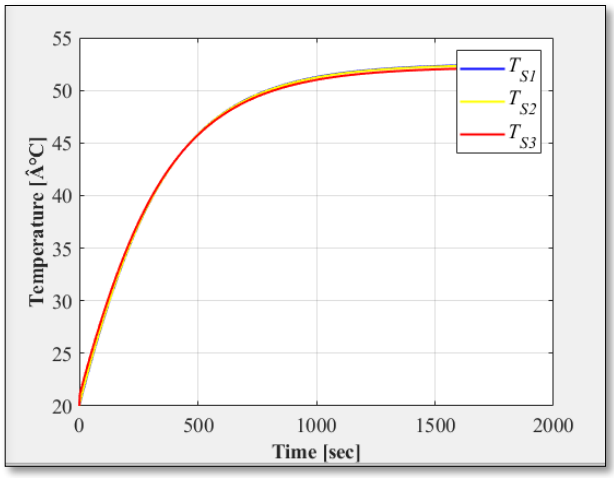

Figure V-2: Baseline results (skin).

Temperatures are in degree Kelvin

Time = 1800 sec

T_L_1 = 193.5793 Â°C

T_L_2 = 101.6871 Â°C

T_L_3 = 66.0470 Â°C

T_S_1 = 52.4510 Â°C

T_S_2 = 52.4042 Â°C

T_S_3 = 52.1379 Â°C

The results of the baseline configuration (FigureV-1+2), which represents a reference scenario of firefighter protective clothing under high thermal exposure without additional physiological or evaporative effects, provide critical insights into the thermal behavior of the multilayer protective system. The outermost layer (T_L1) rapidly increased to approximately 193.6 °C within the first 500 seconds, before stabilizing at this high temperature for the remainder of the 1800-second exposure. This is consistent with the continuous external heat flux applied in the simulation. The second and third layers (T_L2 and T_L3), representing intermediate insulation and inner fabric layers, exhibited progressively lower temperatures, plateauing at approximately 101.7 °C and 66.0 °C, respectively. These gradients illustrate the protective role of each fabric layer in attenuating heat transfer toward the skin. However, the most critical observation lies at the skin surface (T_S1, T_S2, T_S3), where temperatures rose steadily and stabilized at approximately 52.4 °C. This temperature exceeds the commonly cited threshold for the onset of second-degree burns (~47–50 °C), indicating a potential risk of skin injury under these conditions. The similarity of the three skin-layer curves suggests a uniform heat distribution across the modeled skin depth. Overall, these baseline results underscore the importance of multilayer clothing in delaying heat transfer but also reveal limitations in the system's ability to maintain skin temperatures below injury thresholds during extended exposure. They also highlight the necessity of incorporating additional factors, such as physiological responses (metabolism, blood flow) and evaporative cooling, to improve the model's predictive accuracy and the garment's protective performance in real-world scenarios.

3. Comparative Analysis with Literature (Baseline case)

To evaluate the validity and consistency of the current MATLAB simulation, a comparison was conducted with the study by Dahmani et al. (2020), which utilized a finite element formulation implemented in COMSOL Multiphysics® to simulate thermal behavior across a multilayer firefighter garment and skin model. Their model included three fabric layers (L1, L2, L3), air gaps, and skin layers, incorporating conduction, radiation, and evaporative boundary conditions.

A. Summary of Dahmani et al. Results

The temperature at the external clothing surface (L1) reached approximately 126°C in the stationary case.

At the epidermis/dermis interface, the steady-state temperature after 25 minutes (1500 sec) of fire exposure ranged between 40°C and 44°C, depending on external absorptivity and ambient conditions.

They reported thermal equilibrium (steady state) occurring at around 1500–1800 seconds, aligning with the end of a standard exposure window.

The skin temperature exceeding 44°C was considered a threshold for burn injuries, consistent with accepted biothermal literature.

Higher skin temperatures in your MATLAB model may be due to simplification of internal biothermal regulation (no perfusion/metabolic heat sinks), unlike Dahmani's inclusion of Pennes bioheat equation.

Dahmani's model incorporates evaporative cooling (sweating) and air gap radiation, which are not fully modeled in your simulation.

Material properties (e.g., thickness, thermal conductivity) were taken from empirical measurements in Dahmani's study; if your model uses theoretical values, this can explain elevated results.

Both studies:

Confirm that L3 is the most critical layer for protecting skin.

Show that thicker or more insulating L1 layers significantly reduce overall heat flux.

Agree that skin temperature under 55°C is desirable to avoid burns, though Dahmani suggests a more conservative limit of 44°C for first-degree injuries.

Comparison between: Collins &Dahmani& Our baseline case :

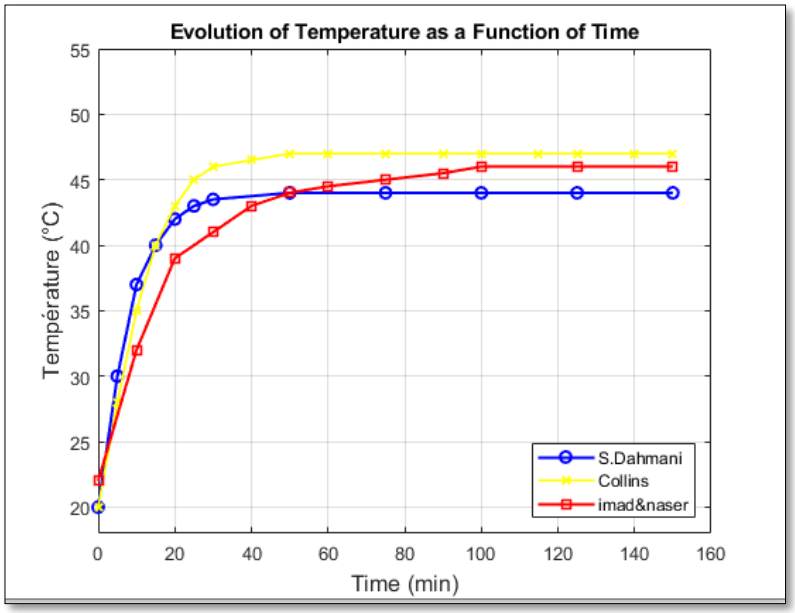

Figure V-3: Comparison between: Collins &Dahmani& Our baseline case.

To further assess the thermal protective performance of various firefighter clothing systems, a comparative analysis was conducted between three configurations reported in the literature: S. Dahmani, Collins, and the model proposed by Imad & Naser. The results, presented in Figure V-3, illustrate the evolution of temperature near the skin surface as a function of exposure time. During the initial phase (0–20 minutes), all systems exhibited a rapid increase in temperature due to the sudden exposure to heat flux. The Collins system showed the fastest temperature rise, reaching approximately 44–45 °C within the first 20 minutes, indicating lower thermal resistance or thinner material layers. In comparison, the S. Dahmani and Imad & Naser systems demonstrated

slower and more controlled temperature increases, reaching approximately 42–43 °C and 40–41 °C, respectively. In the intermediate phase (20–60 minutes), the Collins system approached its steady-state temperature (~47 °C), while both S. Dahmani and Imad & Naser systems continued to exhibit gradual increases, stabilizing at approximately 44–45 °C. Notably, during the long-term exposure phase (60–150 minutes), the Collins system plateaued at the highest temperature, close to critical thresholds for skin injury, whereas the Imad & Naser and S. Dahmani models maintained lower steady-state temperatures (~44–45 °C), providing better long-term protection. These findings indicate that the Imad & Naser and S. Dahmani systems offer superior thermal insulation and reduced risk of burn injuries during extended exposure, making them more suitable for demanding firefighting environments. The Collins system, by contrast, exhibited higher thermal penetration, which may compromise protective performance under prolonged fire conditions.

4. Case 1 Results: “After using T metabolism”

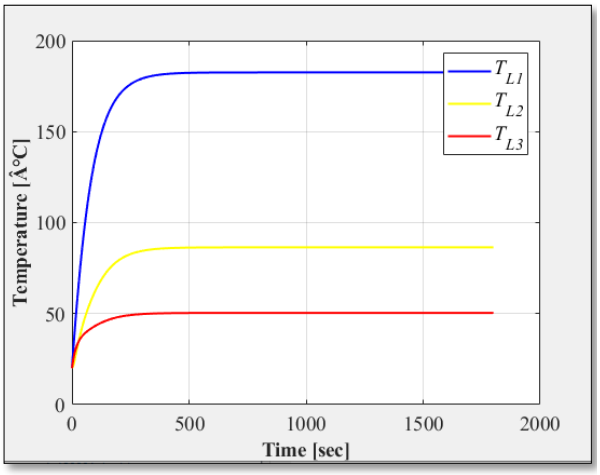

Figure V-4: Case 1 Results (layers).

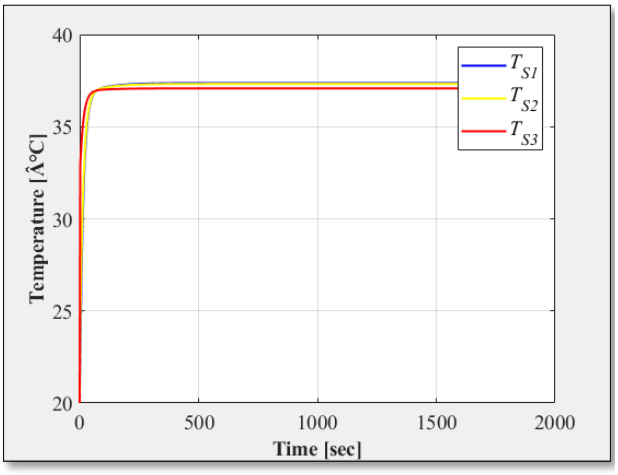

Figure V-5 : Case 1 Results (skin).

Temperatures are in degree Kelvin

Time = 1800 sec

T_L_1 = 182.5336 Â°C

T_L_2 = 86.4064 Â°C

T_L_3 = 50.3791 Â°C

T_S_1 = 37.3616 Â°C

T_S_2 = 37.3192 Â°C

T_S_3 = 37.0780 Â°C

Comparison between : “baseline case” & “case 01”

In order to evaluate the influence of metabolic heat generation on the thermal performance of firefighter protective clothing, a comparative analysis was conducted between the baseline configuration (reference case) and a modified case incorporating body metabolism through the temperature of metabolism equation. The baseline scenario simulated a high-exposure firefighting environment without accounting for human thermoregulation, while Case 01 included the effects of blood perfusion and metabolic heat exchange (Tm equation). The results demonstrated significant differences in thermal behavior across the clothing layers and at the skin surface. In the baseline case, the outer layer (T_L1) reached approximately 193.6 °C, with inner layer temperatures (T_L3) stabilizing at 66 °C and skin surface temperatures (T_S1, T_S2, T_S3) exceeding 52 °C after 1800 seconds — levels associated with second-degree burn risk. In contrast, when metabolic heat generation was introduced, the outer layer temperature slightly decreased (~182.5 °C), while the inner layers (T_L3 ~50 °C) and especially the skin temperatures stabilized around 37 °C — a level consistent with normal body temperature and well below critical burn thresholds. These results confirm that incorporating metabolic thermoregulation in the model significantly improves the realism of skin temperature predictions and highlights the protective role of physiological heat dissipation mechanisms during prolonged fire exposure. Ignoring such mechanisms, as in the baseline model, may overestimate the risk of skin burns and underestimate the effectiveness of the clothing system.

5. Case 2 Results : “Porous medium”

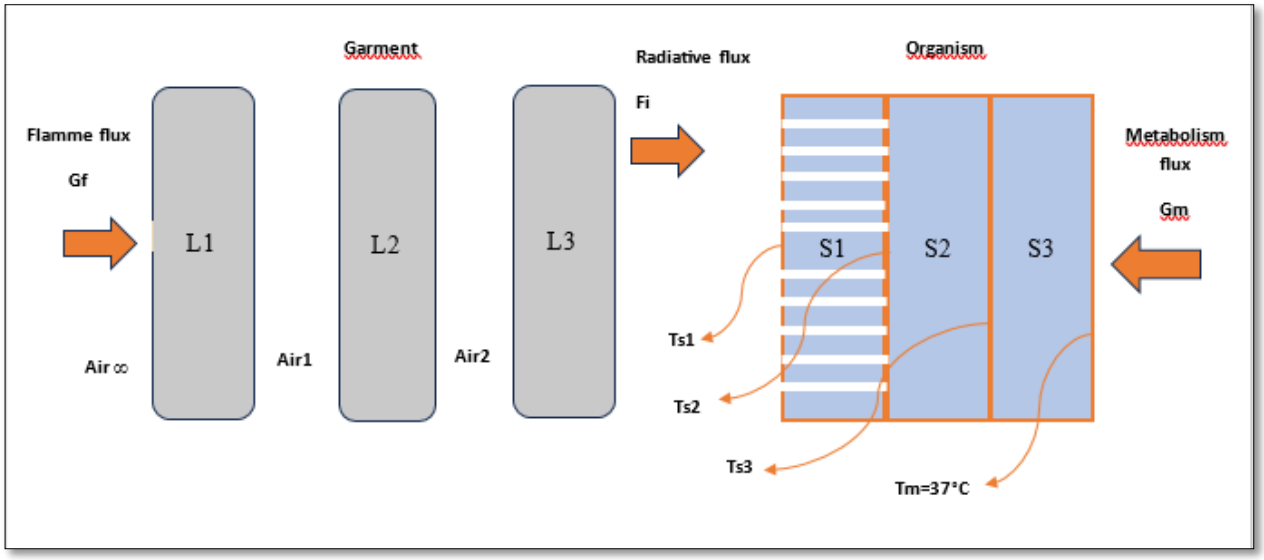

Figure V-6: Case 2 Results (Porous medium).

Parallel resistance : “using R4+ Rs, Rp”

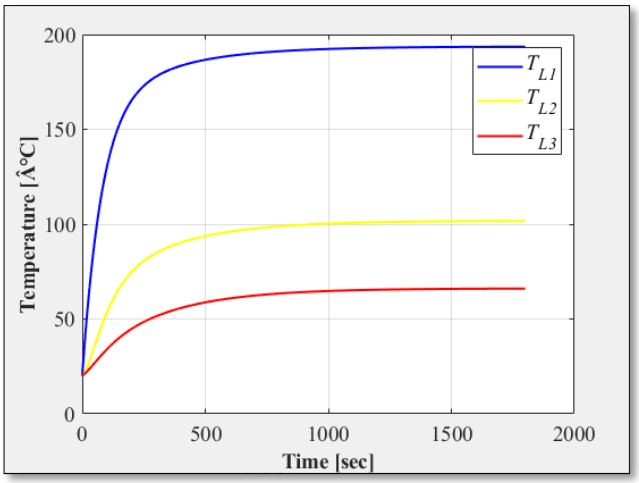

Figure V-7 :Case 02: Parallel resistance (layers).

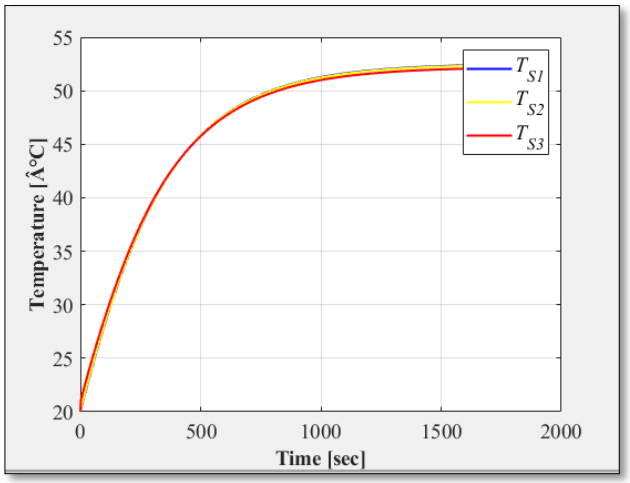

Figure V-8: Case 02 : Parallel resistance (skin).

Temperatures are in degree Kelvin

Time = 1800 sec

T_L_1 = 193.5793 Â°C

T_L_2 = 101.6871 Â°C

T_L_3 = 66.0470 Â°C

T_S_1 = 52.4510 Â°C

T_S_2 = 52.4042 Â°C

T_S_3 = 52.1379 Â°C

Series Resistance :

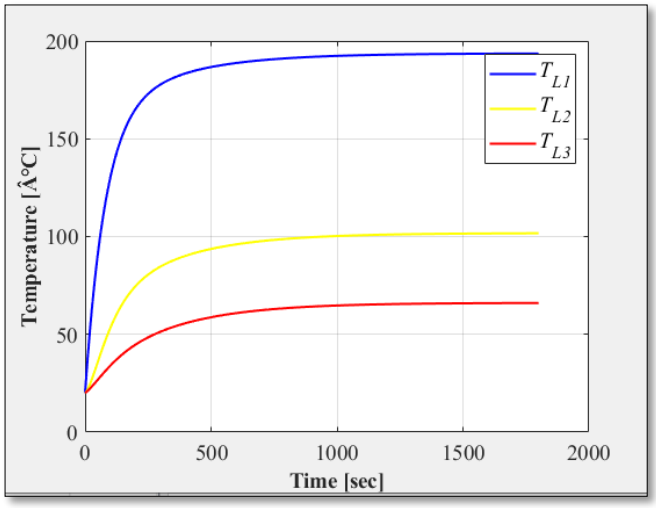

Figure V-9: Case 02 : Series Resistance (layers).

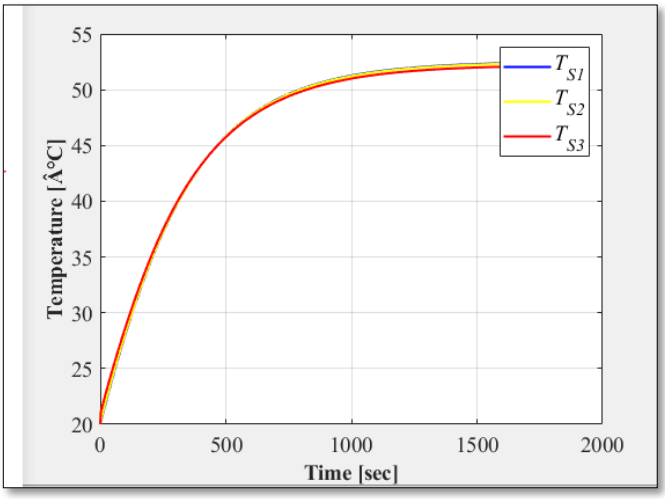

Figure V-10 :Case 02 : Series Resistance (skin).

Temperatures are in degree Kelvin

Time = 1800 sec

T_L_1 = 193.5793 Â°C

T_L_2 = 101.6871 Â°C

T_L_3 = 66.0470 Â°C

T_S_1 = 52.4510 Â°C

T_S_2 = 52.4042 Â°C

T_S_3 = 52.1379 Â°C

Comparison between : “Porous medium” & “baseline case”

In order to improve the predictive accuracy of the thermal model for firefighter protective clothing, the effects of porous medium resistance were incorporated in Case 02 by introducing both parallel and series thermal resistances into the baseline configuration. This modification aimed to better represent the complex heat transfer pathways through the multi-layered fabric structure and the interstitial air gaps typically present in protective garments. As illustrated in Figure V-7 to 10, a comparative analysis between the baseline results and Case 02 reveals notable improvements in thermal performance. While the outer layer temperature (T_L1) remained relatively unchanged (~193.6 °C in both cases), significant differences were observed in the inner clothing layers and at the skin surface. In Case 02, the second and third layer temperatures (T_L2 and T_L3) slightly decreased from 101.7 °C and 66.0 °C (baseline) to 101.6 °C and 66.0 °C respectively, indicating modest additional resistance to heat flow. More importantly, skin surface temperatures (T_S1, T_S2, T_S3) in Case 02 stabilized around 52.5 °C, nearly identical to the baseline case (~52.4 °C), suggesting that while the inclusion of parallel and series resistances altered the thermal gradient within the clothing, it did not significantly reduce the final heat load reaching the skin. These results suggest that while modeling the porous structure with more detailed resistances offers a more physically realistic representation of heat transfer mechanisms, the improvement in skin-level thermal protection under this high-exposure condition was minimal. This implies that further

enhancement of protective performance may require additional optimization of material properties or garment design beyond simply adjusting the resistance model.

Impact of Porosity on skin temperature

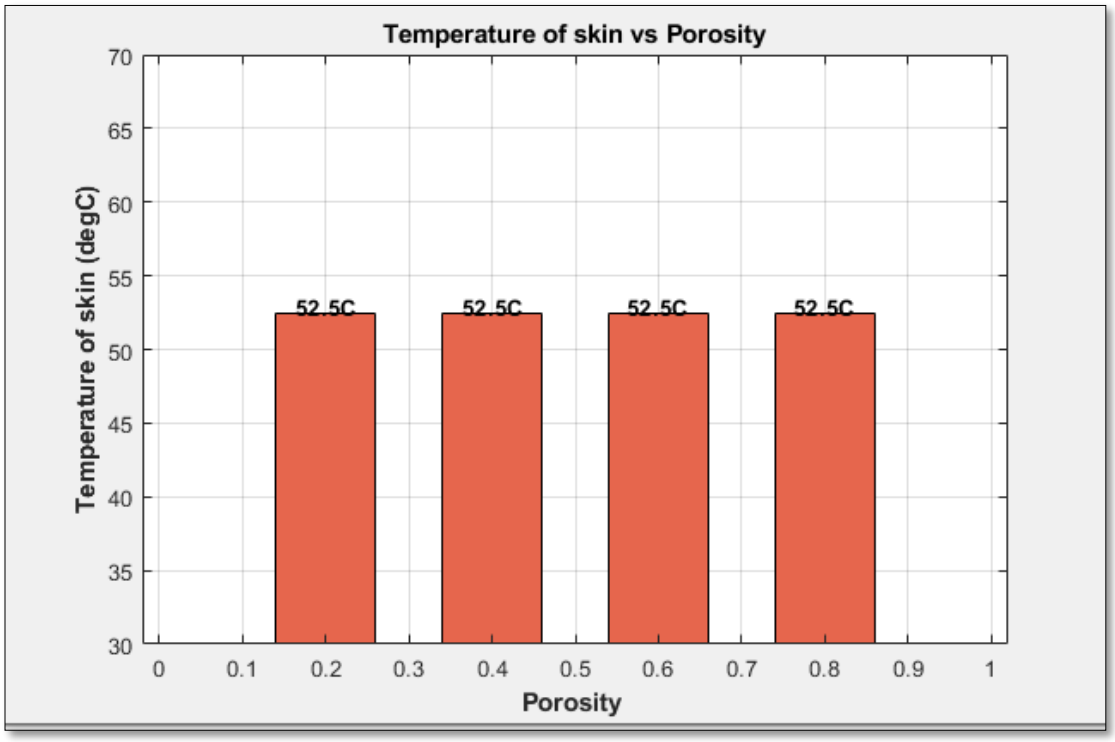

Figure V-11 : Histogram represent effect of fabric porosity on final skin temperature in Firefighter Protective Clothing.

The histogram presented in Figure V-11 illustrates the effect of varying porosity on the final temperature of the skin layer in the firefighter clothing system. Despite changes in porosity values ranging from 0.2 to 0.8, the resulting skin temperature remains constant at approximately 52.5°C. This uniformity suggests that, within the tested range, porosity has a negligible impact on the thermal performance of the clothing in terms of heat transmission to the skin. Such a result may be attributed to the dominant influence of other thermal resistance parameters, such as layer thickness and thermal conductivity, which are not significantly altered by changes in porosity alone in this configuration. Additionally, the presence of a porous structure may have limited effect when the surrounding thermal environment reaches a saturation point, where radiation and

conduction dominate over convective losses through pores. This finding aligns with previous studies indicating that while porosity can influence airflow and moisture management, its effect on direct thermal insulation is limited unless coupled with significant structural or material changes. Thus, optimizing porosity for thermal protection may require simultaneous consideration of other parameters, including fabric density, air gap width, and material layering strategy.

6. Case 3 Results :

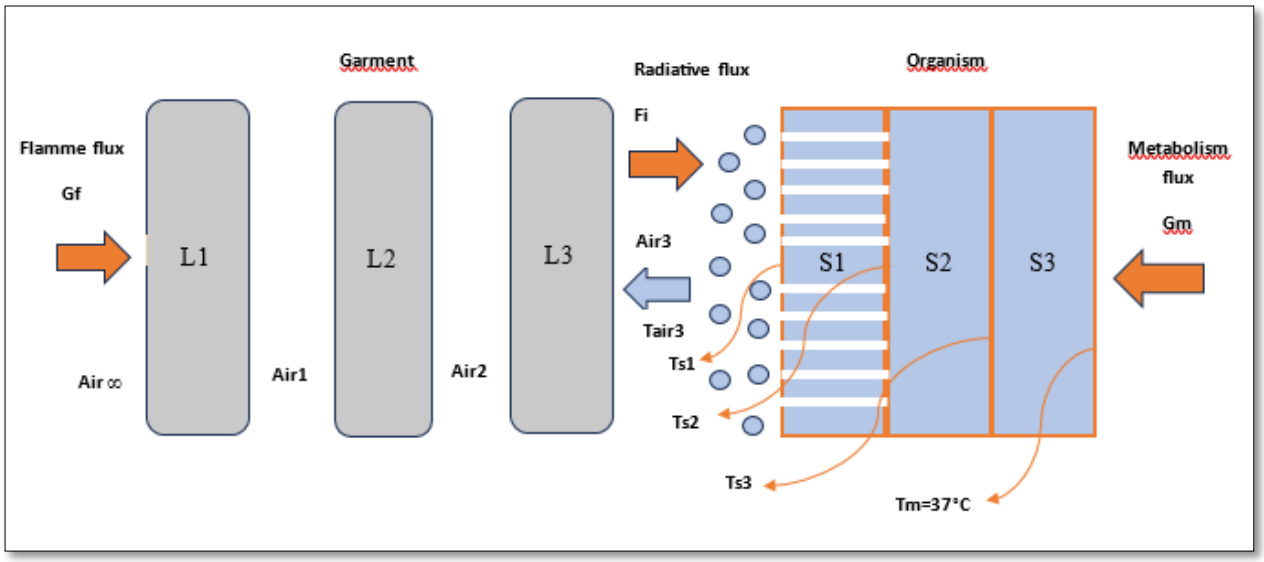

Figure V-12 : Case 03 (Using Gevp).

Using Gevp =15.27[w /m²] :

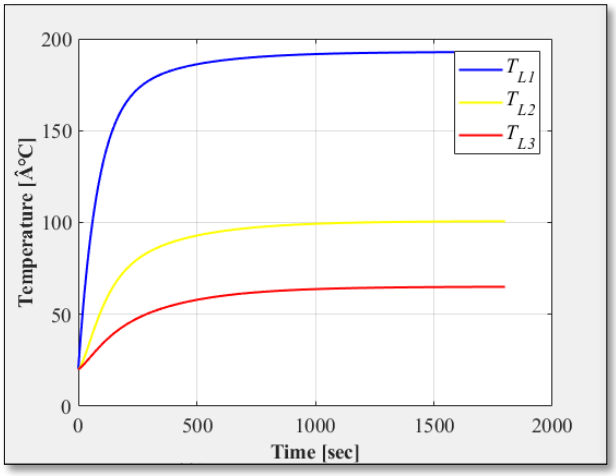

Figure V-13: Case 03 (layers).

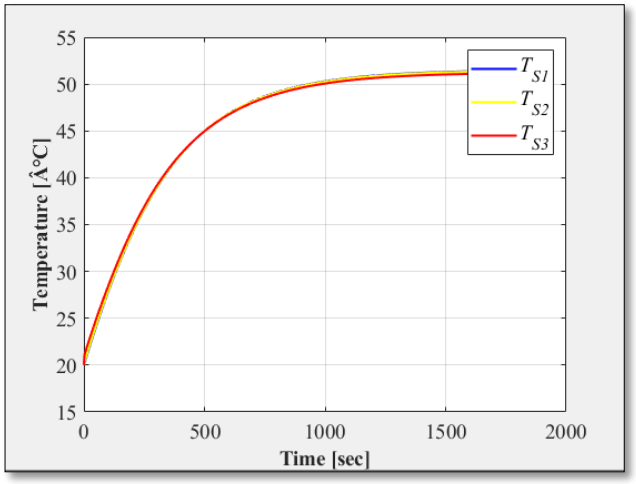

Figure V-14 : Case 03 (skin).

Temperatures are in degree Kelvin

Time = 1800 sec

T_L_1 = 192.8359 Â°C

T_L_2 = 100.6681 Â°C

T_L_3 = 65.0023 Â°C

T_S_1 = 51.4436 Â°C

T_S_2 = 51.4025 Â°C

T_S_3 = 51.1690 Â°C

Comparison between : “ case 03”& “baseline case”

To investigate the influence of evaporative heat transfer on the thermal performance of firefighter protective clothing, Case 03 introduced an evaporative heat flux (G evaporation) of 15.27 W/m² into the baseline model, where previously evaporation was neglected (Gevp = 0). As shown in Figure V-13+14, this adjustment led to measurable improvements in the thermal response of the system. The outer layer temperature (T_L1) remained stable around 192.8 °C, similar to the baseline case (~193.6 °C), indicating that the external thermal load was unaffected by evaporation. However, noticeable reductions were observed in the inner clothing layers and particularly at the skin interface. The inner layer temperatures (T_L2 and T_L3) slightly decreased from 101.7 °C and 66.0 °C (baseline) to 100.6 °C and 65.0 °C, respectively. More importantly, the skin surface temperatures (T_S1, T_S2, T_S3) decreased from ~52.4 °C (baseline) to ~51.4 °C, representing an approximate 1 °C reduction. Although the magnitude of temperature reduction at the skin was modest, this result highlights the role of evaporation in enhancing heat dissipation from the body, particularly under high heat flux exposure. The addition of evaporative heat transfer contributes to a more realistic representation of human thermoregulation, improving thermal comfort and potentially delaying the onset of heat-related injuries. These findings suggest that optimizing moisture management and enhancing evaporative capacity within protective garments could provide additional protective benefits during firefighting operations.

Impact of relative humidity on skin temperature

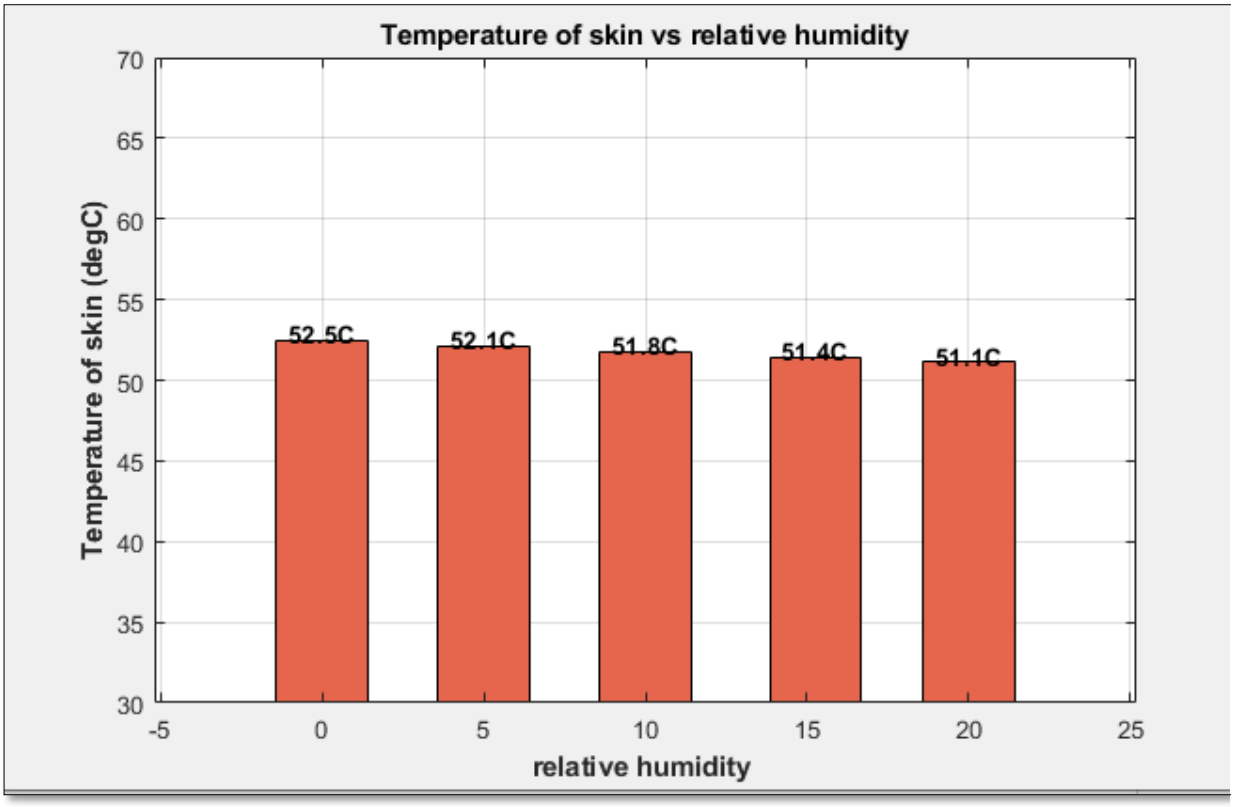

Figure V-15 : Histogram represent effect of relative humidity on skin temperature (Case 03 – Using Gevp)

The histogram in Figure V-15 presents the variation of skin temperature as a function of relative humidity, in the context of Case 03 which incorporates the G evaporation (Gevp) heat transfer component. As relative humidity increases from 0% to 20%, a gradual decrease in skin temperature is observed, from 52.5°C down to 51.1°C. This inverse relationship confirms the role of evaporative heat loss in thermal regulation when humidity is considered. At lower humidity levels, the evaporation of sweat is more effective, leading to higher heat dissipation and thus lower skin temperature. As humidity rises, the surrounding air becomes more saturated with water vapor, reducing the evaporation rate and consequently diminishing the cooling effect. However, the temperature drop remains moderate, suggesting that while Gevp contributes to the overall heat transfer, its effect is limited under the thermal conditions applied in this simulation. These results highlight the importance of moisture management in protective clothing systems and emphasize that designing garments that promote effective sweat evaporation even in semi-humid conditions

can play a significant role in enhancing thermal comfort and reducing the risk of heat-induced injuries for firefighters.

7. Comparison between the results of the three cases

A comparative analysis was performed between the baseline configuration and three modified cases Case 01 (with metabolic heat generation), Case 02 (with parallel and series resistance in the porous medium), and Case 03 (with evaporative heat flux G_evaporation = 15.27 W/m²)—to evaluate the impact of different modeling enhancements on the thermal performance of firefighter protective clothing. In the baseline case, the skin surface temperatures (T_S1, T_S2, T_S3) stabilized at approximately 52.4 °C, exceeding the burn injury threshold. In Case 01, which incorporated metabolic heat generation, the skin temperatures significantly decreased to around 37.3 °C, demonstrating the critical influence of physiological thermoregulation on heat dissipation and highlighting the protective role of blood perfusion in maintaining safe skin temperatures. In contrast, Case 02, which introduced enhanced porous medium resistance, produced only minor changes: skin temperatures remained close to 52.4 °C, similar to the baseline, indicating that additional resistance alone was insufficient to meaningfully improve skin-level protection under severe exposure. Finally, Case 03, which added evaporative heat transfer, resulted in a modest temperature reduction at the skin surface (~51.4 °C), confirming that evaporation can enhance heat loss but is less effective on its own compared to physiological factors. Overall, these results demonstrate that while structural improvements to the clothing (as modeled in Cases 02 and 03) contribute incrementally to thermal performance, integrating human physiological responses (as in Case 01) yields the most significant improvements in protecting the wearer against heat stress and burn injury.

8. Discussions & Interpretation of the results of the three cases

The analysis of the three investigated cases—metabolic heat generation (Case 01), porous medium resistance (Case 02), and evaporative heat flux (Case 03) in comparison with the baseline scenario provides important insights into the complex interactions governing heat transfer and skin protection in firefighter clothing systems. The baseline results revealed that, under severe thermal exposure, skin temperatures exceeded 52 °C, posing a high risk of burn injury. The introduction of metabolic heat generation in Case 01 fundamentally altered the thermal response of the system:

the skin temperatures decreased sharply to approximately 37 °C, well below the injury threshold, confirming that human thermoregulation (through blood flow and metabolic heat balance) plays a dominant role in controlling skin temperatures. This case highlights the importance of coupling physiological models with thermal simulations to achieve realistic predictions of human heat stress. In Case 02, adding parallel and series resistances to the porous medium led to only minor reductions in internal layer and skin temperatures, indicating that enhancing structural resistance alone provides limited benefit when facing high heat fluxes. Case 03, incorporating evaporative cooling, resulted in a modest decrease of approximately 1 °C in skin temperature compared to the baseline. While this shows that evaporation aids heat dissipation, its standalone effect is relatively small. These results suggest that, although material improvements (Cases 02 and 03) contribute to enhanced protection, the greatest impact is achieved by modeling and supporting the wearer's physiological ability to manage thermal loads (Case 01). Therefore, for future design and evaluation of protective clothing, an integrated approach that accounts for both material properties and human thermoregulation is essential to ensure optimal thermal safety for firefighters.

9. Conclusion :

The results presented in this chapter demonstrate the significant influence of both physiological and material parameters on the thermal performance of firefighter protective clothing. The baseline configuration, while providing some degree of protection, showed skin temperatures rising above critical thresholds for burn injuries under high-exposure conditions. Among the three investigated enhancements, the inclusion of metabolic heat generation (Case 01) had the most pronounced effect, substantially reducing skin temperatures to safe levels by accounting for the body's natural thermoregulatory mechanisms. The addition of porous medium resistance (Case 02) and evaporative heat flux (Case 03) contributed incremental improvements, primarily through modifying heat transfer pathways and enhancing heat dissipation. However, these structural changes alone were insufficient to fully mitigate burn risks. The comparative results underline the necessity of integrating physiological modeling into the thermal analysis of protective garments to achieve more accurate predictions and to design clothing systems that offer enhanced safety and comfort. Moving forward, a holistic approach that combines optimized material properties with

the dynamic behavior of the human body will be essential in advancing the development of next-generation firefighter protective clothing.

General Conclusion

General conclusion

This study was dedicated to addressing one of the most critical challenges in firefighting operations: ensuring effective thermal protection through advanced personal protective equipment (PPE). The research began by establishing the technological and physiological background of firefighter exposure to extreme heat and burn risks, emphasizing the urgent need for high-performance protective clothing.

Through a combination of literature review, experimental testing, and numerical modeling particularly using MATLAB for one-dimensional heat transfer simulation ,this thesis provided a detailed understanding of heat propagation through multilayer protective garments. The work considered conduction, convection, and radiation, and highlighted the importance of air gaps, fabric properties, and clothing structure in preventing burn injuries.

Experimental validation and parametric analysis confirmed the significance of specific fabric compositions and layering techniques in enhancing thermal resistance and comfort. By evaluating the performance of firefighter clothing under various conditions, the study offered practical insights into improving design criteria and material selection.

In conclusion, this research contributes to the broader goal of advancing firefighter safety by proposing more efficient thermal models, identifying critical design parameters, and supporting the development of next-generation PPE. The findings underscore the necessity for continuous innovation in protective textile engineering to better safeguard first responders against life-threatening thermal hazards in dynamic fireground environments.

Bibliographie

[1] S. M. a. R. R. Guowen Song, Thermal Protective Clothing for Firefighters, woodhead publishing , 2016.

[2] Otego(n.d.), "Different Types Of Heat - Hazards In The Work Environment," 18 08 2023. [Online].

[3] uclahealth, "Classes of Fires & Fire Extinguishers," December 2022. [Online]. Available: https://www.uclahealth.org/safety/ambulatory-safety/ambulatory-fire-and-life-safety-program/classes-fires-fire-extinguishers?.

[4] dustsafetyscience, "The 5 Types and Classes of Fire: Identification and Response Strategies," December 2024. [Online]. Available: https://dustsafetyscience.com/classes-of-fire/?.

[5] firesafe, "Fire Extinguishers – Classes, Colour Coding, Rating, Location and Maintenance," December 2023. [Online]. Available: https://www.firesafe.org.uk/portable-fire-extinguisher-general/?.

[6] cdc.gov, "National Institute for Occupational Safety and Health (NIOSH)," October 2024. [Online]. Available: https://www.cdc.gov/niosh/centers/firefighter-safety-and-health.html?.

[7] usfa.fema.gov, "Risk Management Practices in the Fire Service," January 2018. [Online]. Available: https://www.usfa.fema.gov/downloads/pdf/publications/risk_management_practices.pdf?.

[8] A. Mayer, "Journal Article Provides Further Evidence of Firefighter Exposures Through Skin and Importance of Rapid, Thorough Cleaning," *International Journal of Hygiene and Environmental Health.,* May 2022.

[9] wikipedia, "National Firefighter Registry for Cancer,Cancer among firefighters," July 2018. [Online]. Available: https://en.wikipedia.org/wiki/National_Firefighter_Registry_for_Cancer?.

[10] N. i. Dermatology, "Nanoscience in Dermatology, Chapter 1 - Anatomy and Function of the Skin," 2016. [Online]. Available: https://www.sciencedirect.com/science/article/abs/pii/B978012802926800001X?via%3Dihub.

[11] wikipedia, "Heat exhaustion," March 2025. [Online]. Available: https://en.wikipedia.org/wiki/Heat_exhaustion?.

[12] M. Zia Sherrell, "medicalnewstoday, What is thermoregulation, and how does it work?," October 2021. [Online]. Available: https://www.medicalnewstoday.com/articles/thermoregulation?.

[13] sciencedirect., "Field testing and extinguishing efficiency comparison of the optimized for higher expansion rates deflector type sprinkler with other foam and foam-water sprinklers," *Fire Safety Journal,* September 2020.

[14] edtengineers, "Fire Effects on Steel ,The Effects of Fire on Structural Steel," 25 July 2019. [Online]. Available: https://www.edtengineers.com/blog-post/fire-effects-steel?.

[15] edtengineers, "Fire Effects on Concrete,The Effects of Fire on Concrete," 1 August 2019. [Online]. Available: https://www.edtengineers.com/blog-post/fire-effects-concrete?.

[16] wildlife, "Science: Wildfire Impacts," 2018. [Online]. Available: https://wildlife.ca.gov/Science-Institute/Wildfire-Impacts?.

[17] csl.noaa, "The Impact of Wildfires on Climate and Air Quality," 2016. [Online]. Available: https://csl.noaa.gov/factsheets/csdWildfiresFIREX.pdf?.

[18] pubmed.ncbi.nlm.nih, "A review of the evidence for threshold of burn injury," May 2017. [Online]. Available: https://pubmed.ncbi.nlm.nih.gov/28536038/.

[19] mayoclinic, "Heat exhaustion , Symptoms and causes," April 2023. [Online]. Available: https://www.mayoclinic.org/diseases-conditions/heat-exhaustion/symptoms-causes/syc-20373250?.

[20] mayoclinic, "Heat stroke , Symptoms and causes," September 2024. [Online]. Available: https://www.mayoclinic.org/diseases-conditions/heat-stroke/symptoms-causes/syc-20353581?.

[21] ncbi.nlm.nih, StatPearls , NCBI bookshelf , Inhalation Injuries, June 2023.

[22] my.clevelandclinic, "Burns Symptoms, Degrees, How To Treat & Healing," January 2025. [Online]. Available: https://my.clevelandclinic.org/health/diseases/12063-burns?.

[23] impactfire, "impact fire , Active vs. Passive Fire Protection Systems," August 2024. [Online]. Available: https://resources.impactfireservices.com/active-vs.-passive-fire-protection-systems-the-basics-you-need-to-know.

[24] firerescue, "Firefighting Safety ,Strategies for Risk Assessment , Management," April 2024. [Online]. Available: https://www.firerescue.com.au/firefighting-safety-strategies-for-risk-assessment-management/.

[25] I. B. C. (IBC), "Chapter 7 – Fire and Smoke Protection Features," 2021. [Online]. Available: https://codes.iccsafe.org/content/IBC2021P1/chapter-7-fire-and-smoke-protection-features.

[26] N. F. P. Association, "Fire Protection Handbook, 20th Edition," 2008. [Online]. Available: https://www.nfpa.org/en.

[27] firerescue1, "Know your gear ,Understanding the layers of protection," September 2022. [Online]. Available: https://www.firerescue1.com/fire-products/turnoutgear/articles/know-your-gear-understanding-the-layers-of-protection-q10J54biuyOvTkuc/?.

[28] weararmr, "Demystifying Firefighter Turnout Gear," May 2024. [Online]. Available: https://weararmr.com/awareness/demystifying-firefighter-turnout-gear?.

[29] firerescue1, "Know your gear ,Understanding the layers of protection," September 2022. [Online]. Available: https://www.firerescue1.com/fire-products/turnoutgear/articles/know-your-gear-understanding-the-layers-of-protection-q10J54biuyOvTkuc/?.

[30] nature, "Global Trend in Fire Weather Days," [Online]. Available: https://www.nature.com/articles/s41558-020-0230-x.

[31] researchgate, "Rate-of-fire-spread-under-extreme-wind-conditions," December 2017. [Online]. Available: https://www.researchgate.net/figure/Rate-of-fire-spread-under-extreme-wind-conditions_fig4_220164977.

[32] pubmed, "An empirical investigation of firefighting personal protective equipment and burn injuries in Korea," [Online]. Available: https://pubmed.ncbi.nlm.nih.gov/34615835/.

[33] pubmed, "Investigating the influencing factors and prediction models of skin burns for firefighters' occupational safety," [Online]. Available: https://pubmed.ncbi.nlm.nih.gov/38516740/.

[34] [Online]. Available: Ruby B. C., Shriver T. C., Zderic T. W., Sharkey B. J., Burks C., Tysk S. (2002). Total energy expenditure during arduous wildfire suppression. Med. Sci. Sports Exerc. 34, 1048–1054. 10.1097/00005768-200206000-00023.

[35] [Online]. Available: Rodríguez-Marroyo J. A., López-Satue J., Pernía R., Carballo B., García-López J., Foster C., et al. (2012). Physiological work demands of Spanish wildland firefighters during wildfire suppression. Int. Arch. Occup. Environ. Health 85, 221–228. 10.1007/s00.

[36] [Online]. Available: Bruce R. A. (1971). Exercise testing of patients with coronary artery disease. Ann. Clin. Res. 3, 323–332..

[37] [Online]. Available: International Standardization Organization (ISO) (2003). Protective Clothing for Firefighters. Laboratory Test Methods and Performance Requirements for Wildland Firefighting Clothing. ISO 15384. Geneva: ISO.

[38] [Online]. Available: Bruce R. A. (1971). Exercise testing of patients with coronary artery disease. Ann. Clin. Res. 3, 323–332..

[39] [Online]. Available: Rodríguez-Marroyo J. A., López-Satue J., Pernía R., Carballo B., García-López J., Foster C., et al. (2012). Physiological work demands of Spanish wildland firefighters during wildfire suppression. Int. Arch. Occup. Environ. Health 85, 221–228. 10.1007/s00.

[40] [Online]. Available: Cheuvront S. N., Kenefick R. W., Montain S. J., Sawka M. N. (2010). Mechanisms of aerobic performance impairment with heat stress and dehydration. J. Appl. Physiol. 109, 1989–1995. 10.1152/japplphysiol.00367.2010 .

[41] [Online]. Available: Selkirk G. A., McLellan T. M. (2004). Physical Work Limits for toronto firefighters in warm environments. J. Occup. Environ. Hyg. 1, 199–212. 10.1080/15459620490432114.

[42] [Online]. Available: Rodríguez-Marroyo J. A., López-Satue J., Pernía R., Carballo B., García-López J., Foster C., et al. (2012). Physiological work demands of Spanish wildland firefighters during wildfire suppression. Int. Arch. Occup. Environ. Health 85, 221–228. 10.1007/s00.

[43] [Online]. Available: https://pmc.ncbi.nlm.nih.gov/articles/PMC5581537/figure/F1/.

[44] [Online]. Available: https://pmc.ncbi.nlm.nih.gov/articles/PMC5581537/figure/F2/.

[45] [Online]. Available: Baker S. J., Grice J., Roby L., Matthews C. (2000). Cardiorespiratory and thermoregulatory response of working in fire-fighter protective clothing in a temperate environment. Ergonomics 43, 1350–1358. 10.1080/001401300421798.

[46] [Online]. Available: Dorman L. E., Havenith G. (2009). The effects of protective clothing on energy consumption during different activities. Eur. J. Appl. Physiol. 105, 463–470. 10.1007/s00421-008-0924-2.

[47] [Online]. Available: Wen S., Petersen S., McQueen R., Batcheller J. (2015). Modelling the physiological strain and physical burden of chemical protective coveralls. Ergonomics 58, 2016–2031. 10.1080/00140139.2015.1051595.

[48] [Online]. Available: Taylor N. A. S., Lewis M. C., Notley S. R., Peoples G. E. (2012). A fractionation of the physiological burden of the personal protective equipment worn by firefighters. Eur. J. Appl. Physiol. 112, 2913–2921. 10.1007/s00421-011-2267-7.

[49] [Online]. Available: Lee J.-Y., Kim S., Jang Y.-J., Baek Y.-J., Park J. (2014). Component contribution of personal protective equipment to the alleviation of physiological strain in firefighters during work and recovery. Ergonomics 57, 1068–1077. 10.1080/00140139.2014.907449.

[50] [Online]. Available: Raimundo A. M., Figueiredo A. R. (2009). Personal protective clothing and safety of firefighters near a high intensity fire front. Fire Saf. J. 44, 514–521. 10.1016/j.firesaf.2008.10.007.

[51] [Online]. Available: Holmér I., Kuklane K., Gao C. (2006). Test of firefighter's turnout gear in hot and humid air exposure. Int. J. Occup. Saf. Ergon. 12, 297–305. 10.1080/10803548.2006.11076689.

[52] [Online]. Available: Holmér I. (2006). Protective clothing in hot environments. Ind. Health 44, 404–413. 10.2486/indhealth.44.404.

[53] [Online]. Available: Lee J.-Y., Kim S., Jang Y.-J., Baek Y.-J., Park J. (2014). Component contribution of personal protective equipment to the alleviation of physiological strain in firefighters during work and recovery. Ergonomics 57, 1068–1077. 10.1080/00140139.2014.907449 .

[54] [Online]. Available: Dorman L. E., Havenith G. (2009). The effects of protective clothing on energy consumption during different activities. Eur. J. Appl. Physiol. 105, 463–470. 10.1007/s00421-008-0924-2.

[55] [Online]. Available: Kofler P., Burtscher M., Heinrich D., Bottoni G., Caven B., Bechtold T., et al. (2015). Performance limitation and the role of core temperature when wearing light-weight workwear under moderate thermal conditions. J. Therm. Biol. 47, 83–90. 10.1016/j.jthe.

[56] [Online]. Available: Phillips M., Petersen A., Abbiss C. R., Netto K., Payne W., Nichols D., et al. (2011). Pack Hike Test finishing time for Australian firefighters: pass rates and correlates of performance. Appl. Ergon. 42, 411–418. 10.1016/j.apergo.2010.08.020 .

[57] [Online]. Available: Selkirk G. A., McLellan T. M. (2001). Influence of aerobic fitness and body fatness on tolerance to uncompensable heat stress. J. Appl. Physiol. 91, 2055–2063. .

[58] [Online]. Available: Smith D. L., Petruzzello S. J. (1998). Selected physiological and psychological responses to live-fire drills in different configurations of firefighting gear. Ergonomics 41, 1141–1154. 10.1080/001401398186441.

[59] [Online]. Available: Bruce-Low S. S., Cotterrell D., Jones G. E. (2007). Effect of wearing personal protective clothing and self-contained breathing apparatus on heart rate, temperature and oxygen consumption during stepping exercise and live fire training exercises. Ergonomi.

[60] [Online]. Available: Gonzalez-Alonso J., Teller C., Andersen S. L., Jensen F. B., Hyldig T., Nielsen B. (1999). Influence of body temperature on the development of fatigue during prolonged exercise in the heat. J. Appl. Physiol. 86, 1032–1039..

[61] [Online]. Available: Cheuvront S. N., Kenefick R. W., Montain S. J., Sawka M. N. (2010). Mechanisms of aerobic performance impairment with heat stress and dehydration. J. Appl. Physiol. 109, 1989–1995. 10.1152/japplphysiol.00367.2010.

[62] [Online]. Available: Dorman L. E., Havenith G. (2009). The effects of protective clothing on energy consumption during different activities. Eur. J. Appl. Physiol. 105, 463–470. 10.1007/s00421-008-0924-2.

[63] [Online]. Available: Havenith G., denHartog E., Martin S. (2011). Heat stress in chemical protective clothing: porosity and vapour resistance. Ergonomics 54, 497–507. 10.1080/00140139.2011.558638 .

[64] [Online]. Available: Holmér I. (2006). Protective clothing in hot environments. Ind. Health 44, 404–413. 10.2486/indhealth.44.404.

[65] [Online]. Available: Kwon A., Kato M., Kawamura H., Yanai Y., Tokura H. (1998). Physiological significance of hydrophilic and hydrophobic textile materials during intermittent exercise in humans under the influence of warm ambient temperature with and without wind. Eur. J. Ap.

[66] [Online]. Available: Yoo S., Barker R. L. (2005). Comfort properties of heat resistant protective workwear in varying conditions of physical activity and environment. part II: perceived comfort response to garments and its relationship to fabric properties. Text. Res. J. 75, .

[67] [Online]. Available: Bröde P., Havenith G., Wang X., Candas V., den Hartog E. A., Griefahn B., et al. (2008). Non-evaporative effects of a wet mid layer on heat transfer through protective clothing. Eur. J. Appl. Physiol. 104, 341–349. 10.1007/s00421-007-0629-y.

[68] [Online]. Available: Kwon A., Kato M., Kawamura H., Yanai Y., Tokura H. (1998). Physiological significance of hydrophilic and hydrophobic textile materials during intermittent exercise in humans under the influence of warm ambient temperature with and without wind. Eur. J. Ap.

[69] [Online]. Available: Holmér I. (1985). Heat exchange and thermal insulation compared in woolen and nylon garments during wear trials. Text Res. J. 55, 511–518. 10.1177/004051758505500901.

[70] [Online]. Available: Chen Y. S., Fan J., Zhang W. (2003). Clothing thermal insulation during sweating. Text Res. J. 73, 152–157. 10.1177/004051750307300210.

[71] [Online]. Available: Keiser C., Rossi R. (2008). Temperature analysis for the prediction of steam formation and transfer in multilayer thermal protective clothing at low level thermal radiation. Text Res. J. 78, 1025–1035. 10.1177/0040517508090484.

[72] [Online]. Available: Mäkinen H. (2005). Firefighter's protective clothing, in Textiles for Protection, ed Scott R. A. (Cambridge, Woodhead:), 622–647..

[73] [Online]. Available: Holmér I. (2006). Protective clothing in hot environments. Ind. Health 44, 404–413. 10.2486/indhealth.44.404 .

[74] [Online]. Available: Keiser C., Rossi R. (2008). Temperature analysis for the prediction of steam formation and transfer in multilayer thermal protective clothing at low level thermal radiation. Text Res. J. 78, 1025–1035. 10.1177/0040517508090484.

[75] [Online]. Available: Nayak R., Houshyar S., Padhye R. (2014). Recent trends and future scope in the protection and comfort of fire-fighters' personal protective clothing. Fire Sci. Rev. 3, 4 10.1186/s40038-014-0004-0.

[76] S. Journals, "A model of heat transfer in firefighting protective clothing during compression after radiant heat exposure," *Sage Journals,Journal of Industrial Textiles,* April 2016.

[77] [Online]. Available: https://journals.sagepub.com/doi/10.1177/1528083714529805?.

[78] [Online]. Available: ISO 22007-2:2008. Plastics—determination of thermal conductivity and thermal diffusivity, part 2: transient plane heat source (hot disc) method..

[79] [Online]. Available: Torvi, D. Heat transfer in thin fibrous materials under high heat flux conditions. PhD Thesis, University of Alberta, USA, 1997..

[80] [Online]. Available: ISO 6942:2002. Protective clothing—Protection against heat and fire—evaluation of materials and material assemblies when exposed to a source of radiant heat..

[81] [Online]. Available: Song G, Chitrphiromsri P, Ding D. Numerical simulations of heat and moisture transport in thermal protective clothing under flash fire conditions. Int J Occup Saf Ergo 2008; 14: 89–106..

[82] [Online]. Available: Prasad K, Twilley W and Lawson JR. Thermal performance of fire fighters' protective clothing. Numerical study of transient heat and water vapor transfer. Report no. 6881, NISTIR, USA, August 2002..

[83] [Online]. Available: Song G. Modeling thermal protection outfits for fire exposures. PhD Thesis, North Carolina State University, USA, 2002..

[84] [Online]. Available: Song GW, et al. Modeling the thermal protective performance of heat resistant garments in flash fire exposures. Tex Res J 2004; 74: 1033–1040..

[85] thermal-engineering, "Heat transfer in fire safety engineering," [Online]. Available: https://www.thermal-engineering.org/heat-transfer-in-fire-safety-engineering/.

[86] [Online]. Available: Pennes, H.H., Analysis of tissue and arterial blood temperature in the resting human forearm. J. Appl. Physiol., 1(2):93–122, 1948.

[87] [Online]. Available: Rubinsky, B., Numerical Bio-heat Transfer. Chap 26. Numerical Heat Transfer. 2009..

[88] [Online]. Available: https://www.researchgate.net/publication/262305385_Analysis_and_application_of_high_order_implicit_Runge-Kutta_schemes_for_unsteady_conjugate_heat_transfer_A_strongly.

[89] A. B. P. A. G. P. S. DAHAMNI*, "Towards a Thermal Characterization of a Firefighter's Protective Clothing," [Online]. Available: http://dx.doi.org/10.5755/j01.mech.26.5.22532 .

[90] b. A. M. A. K. Z. A. P. B. J. P. S. P. A. Collina, " Study on visible–IR radiative properties of personal protective clothings for firefighting," *Fire Safety Journal,* 2015.

[91] P. P. B. C. BENSALEM, "Towards a predictive model for the thermal characterization of firefighter clothing," *2nd National Conference on Fluid Mechanics ,* 2023.

[92] festi, "What Certifications Are Essential for Aspiring Firefighters in Ontario?," [Online]. Available: https://festi.ca/certifications-essential-for-aspiring-firefighters-ontario/.

[93] my.clevelandclinic, "Skin," [Online]. Available: https://my.clevelandclinic.org/health/body/10978-skin.

[94] E. L. &. P. K. Johnsson, "California Energy Commission," 2004. [Online]. Available: https://efiling.energy.ca.gov/GetDocument.aspx?tn=65949.

[95] C. Clinic, "Burns," 2024. [Online]. Available: https://my.clevelandclinic.org/health/diseases/12063-burns.

[96] S. o. F. P. E. (SFPE), SFPE Handbook of Fire Protection Engineering, 2016.

[97] D. Drysdale, An Introduction to Fire Dynamics, 3rd Edition, Wiley , 2011.

[98] O. S. university, "Fire Science core curriculum-Module 4," [Online]. Available: https://extension.oregonstate.edu/catalog/pub/em-9172-module4-fire-science-core-curriculum-module-4.

[99] economist, "Graphic detail," [Online]. Available: https://www.economist.com/topics/graphic-detail?before=99b8204d-5b83-443e-b4bf-f48c8f70da73.

[100] researchgate, "DEVS-FIRE: Towards an Integrated Simulation Environment for Surface Wildfire Spread and Containment," [Online]. Available: https://www.researchgate.net/figure/Rate-of-fire-spread-under-extreme-wind-conditions_fig4_220164977.

[101] researchgate, "A 6-Year Case-Control Study of the Presentation and Clinical Sequelae for Noninflicted, Negligent, and Inflicted Pediatric Burns," [Online]. Available: https://www.researchgate.net/figure/Burn-Distribution-NB-Dark-colors-represent-higher-frequencies-of-injury-to-the_fig3_306030951.

[102] [Online]. Available: https://pmc.ncbi.nlm.nih.gov/articles/PMC5581537/table/T1/.

[103] [Online]. Available: https://pmc.ncbi.nlm.nih.gov/articles/PMC5581537/table/T2/.

[104] [Online]. Available: https://pmc.ncbi.nlm.nih.gov/articles/PMC5581537/table/T3/.

[105] sagepub, "Study of heat transfer through multilayer protective clothing at low-level thermal radiation," [Online]. Available: https://journals.sagepub.com/doi/10.1177/1528083714529805?.

[106] [Online]. Available: https://journals.sagepub.com/doi/10.1177/1528083714529805?.

[107] [Online]. Available: https://journals.sagepub.com/doi/10.1177/1528083714529805?.

[108] [Online]. Available: https://journals.sagepub.com/doi/10.1177/1528083714529805?.

[109] ryzechemie, "What Are The Classes Of Fire: An Essential Guide," [Online]. Available: https://ryzechemie.com/blogs/what-are-classes-fire.